Volume 8 | Number 13 | 7 April 2016 | Pages 6887–7354

Nanoscale

www.rsc.org/nanoscale

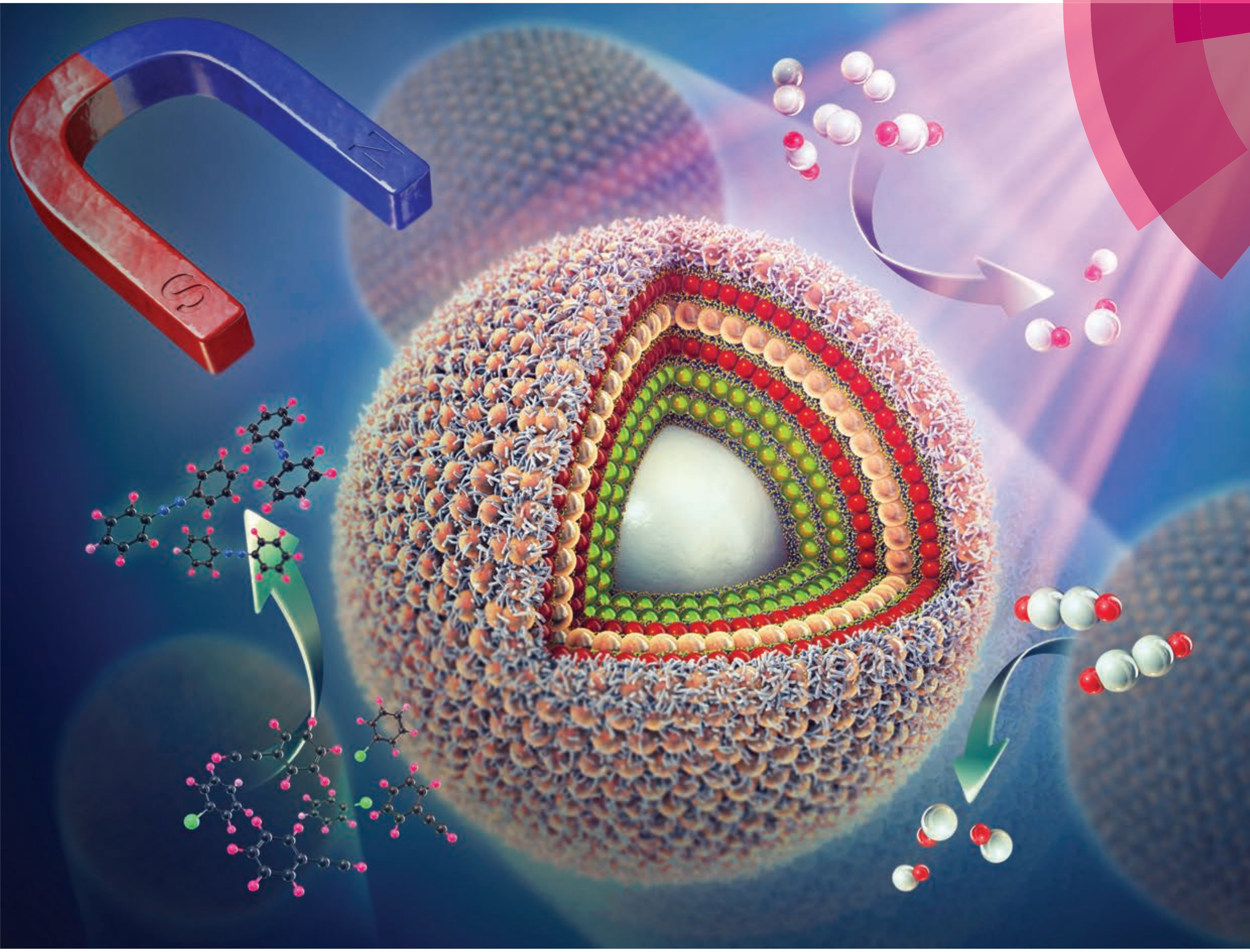

ISSN 2040-3364

ROYAL SOCIETY OF CHEMISTRY

PAPER
Jai-Kyeong Kim, Jinhan Cho *et al.*
Multicatalytic colloids with highly scalable, adjustable, and stable functionalities in organic and aqueous media

NCNST

Nanoscale

PAPER

View Article Online
View Journal | View Issue

Cite this: *Nanoscale*, 2016, **8**, 7000

Published on 19 October 2015. Downloaded by Korea University on 26/03/2016 04:39:26.

Multicatalytic colloids with highly scalable, adjustable, and stable functionalities in organic and aqueous media†

Donghee Kim,[a] Sanghyuk Cheong,[a] Yun Gyong Ahn,[b] Sook Won Ryu,[c] Jai-Kyeong Kim*[d] and Jinhan Cho*[a]

Despite a large number of developments of noble metal (or metal oxide) NP-based catalysts, it has been a great challenge to prepare high-performance recyclable catalysts with integrated functionalities that can be used in various solvent media. Here, we report on layer-by-layer (LbL) assembled multicatalysts with high catalytic performance, showing high dispersion and recycling stability in organic and aqueous media. The remarkable advantages of our approach are as follows. (i) Various metal or metal oxide NPs with desired catalytic performance can be easily incorporated into multilayered shells, forming densely packed arrays that allow one colloid to be used as a multicatalyst with highly integrated and controllable catalytic properties. (ii) Additionally, the dispersion stability of catalytic colloids in a desired solvent can be determined by the type of ultrathin outermost layer coating each colloid. (iii) Lastly, the covalent bonding between inorganic NPs and dendrimers within multilayer shells enhances the recycling stability of multicatalytic colloids. The resulting core–shell colloids including OA–Fe_3O_4 NPs, TOABr–Pd NPs, and OA–TiO_2 NPs exhibited excellent performance in the oxidation of 3,3′,5,5′-tetramethylbenzidine (TMB) and photocatalysis in aqueous media and in the Sonogashira coupling reaction (99% yield) in organic media. Given that the catalytic properties of recyclable colloids reported to date have entirely depended on the functionality of a single catalytic NP layer deposited onto colloids in selective solvent media, our approach provides a basis for the design and exploitation of high-performance recyclable colloids with integrated multicatalytic properties and high dispersion stability in a variety of solvents.

Received 16th September 2015,
Accepted 12th October 2015

DOI: 10.1039/c5nr06390f

www.rsc.org/nanoscale

1. Introduction

Nanocomposite colloids hold immense promise for revolutionizing various academic and industrial fields such as photonics,[1,2] sensing,[3] membranes,[4] diagnosis,[5,6] medicine,[7] and catalysis.[5,8] Recent advances in nanoscience and colloidal technology have strongly driven the development of colloids with integrated and multifunctional properties; currently, versatile and robust approaches are required to integrate these properties into engineering materials. In particular, nanocomposite colloids containing noble metal (or metal oxide) and iron oxide nanoparticles (NPs) have attracted considerable attention because of their potential for use as reusable catalysts in the organic synthetic, biocatalytic, and water-purification industries. Several crucial factors must be considered for the preparation of such functional colloids. First, the catalytic metal or metal oxide NPs should be designed so that their catalytic activity is strongly influenced by the NP size and crystallinity.[9–11] Considering that various hydrophobic ligands (*e.g.*, oleic acid (OA), linoleic acid or tetraoctylammonium bromide (TOABr)) can yield large concentrations of catalytic NPs in nonpolar solvents, the synthesis of metal or metal oxide NPs using hydrophobic ligands in nonpolar media is more desirable compared to the NP synthesis in aqueous media, which is associated with relatively poor quality and dilute concentration. Second, a variety of catalytic NPs with desired functionalities should be densely coated onto the surface of colloids because the loading quantity of catalytic NPs onto colloids is directly related to the overall catalytic activity of each type of nanocomposite colloid. To this end,

---

[a] *Department of Chemical & Biological Engineering, Korea University Anam-dong, Seongbuk-gu, Seoul 136-713, Republic of Korea. E-mail: jinhan71@korea.ac.kr*
[b] *Western Seoul Center, Korea Basic Science Institute Bugahyeon-ro, Seodaemun-gu, Seoul 120-140, Republic of Korea*
[c] *Department of Laboratory Medicine, Kangwon National University School of Medicine Kangwondaehak-gil, Chuncheon-si, Gangwon-do 200-701, Republic of Korea*
[d] *Photoelectronic Hybrid Research Center, Korea Institute of Science and Technology Hwarang-ro 14-gil, Seongbuk-gu, Seoul 136-791, Republic of Korea. E-mail: jack@kist.re.kr*

† Electronic supplementary information (ESI) available: The ATR-FTIR spectra, SEM images, TEM images, UV-Vis spectra, and magnetism curves. See DOI: 10.1039/c5nr06390f

This journal is © The Royal Society of Chemistry 2016

Published on 19 October 2015. Downloaded by Korea University on 26/03/2016 04:39:26.

polymers with thiol moieties should not be used as a binding linker for the adsorption of catalytic metal NPs onto colloidal substrates because thiol moieties that are strongly bound to the surface of metal NPs significantly decrease the catalytic activity of the metal (*e.g.*, Au, Pt, or Pd) NPs.[12] Third, to achieve cost-effectiveness, it is desirable that precious catalysts, including the above-mentioned noble metal NPs, should be recyclable and reusable in various solvent media.

Efforts to prepare recyclable catalytic colloids have employed a variety of approaches, such as surface-initiated controlled polymerization,[13] emulsification,[14] sonochemistry,[15] sol–gel processing,[16–18] and direct NP adsorption.[19] However, these approaches have much difficulty in realizing more than one catalytic property at the single-colloid level due to the use of a single catalytic NP layer with a relatively low loading amount of NPs. Additionally, they have limited a stable dispersion of catalytic colloids in various solvent media. As a result, these previous approaches have encountered challenges in controlling or improving catalytic functionality in any given catalytic colloid system.

Among the various approaches for the preparation of functional colloids, it has been demonstrated that the layer-by-layer (LbL) assembly approach[2,3,20–32] is versatile and offers the opportunity to prepare organic/metal (or metal oxide) nanocomposite films with controlled thickness and composition on substrates of various sizes and shapes. The dispersion stability, functionality, and performance of LbL-assembled multilayer-coated colloids strongly depend on the surface polarity of the outermost layer, the inherent properties, and the loading amount of the coating components, respectively. These LbL-assembled colloids have mainly been prepared by exploiting the electrostatic interaction between oppositely charged components in aqueous media. However, in the case of electrostatic LbL-assembled colloids, electrostatic repulsion among the same charged NPs decreases the loading amount of functional NPs adsorbed onto colloids,[25] which constitutes a major obstacle in enhancing the overall performance of catalytic colloids. In addition, catalytic colloids prepared *via* electrostatic LbL assembly cannot be directly utilized in organic synthesis processes or petrochemical industries, which require high dispersion stability in organic media.

Here, we report for the first time that recyclable colloids with scalable and adjustable multicatalytic properties in various solvent media can be prepared using LbL assembly between catalytic NPs and dendrimers. The importance of our work lies in the fact that the proposed strategy can be effectively applied to catalysts requiring high performance, and integrated and tailored functionalities in various solvent media. As model systems for this study, Pd,[33,34] TiO_2,[35,36] and Fe_3O_4 NPs[37] were selected because they have been widely used as representative NPs for various catalytic reactions and magnetically retrievable materials. These hydrophobic NPs (termed TOABr–Pd, OA–TiO_2, and OA–Fe_3O_4 NPs) were LbL-assembled with amine-functionalized dendrimers (NH_2–dendrimers) onto SiO_2 colloids using a ligand-exchange reaction between the TOABr and OA ligands loosely bound to the surface of the inorganic NPs and the NH_2 groups of the dendrimers. The resulting nanocomposite colloids exhibited excellent multicatalytic properties as demonstrated by 3,3′,5,5′-tetramethylbenzidine (TMB) oxidation by TOABr–Pd NP layers in aqueous media, by the Sonogashira coupling reaction by TOABr–Pd NP layers in organic media, and by photocatalysis by OA–TiO_2 NP layers in aqueous media (Scheme 1). The performance of

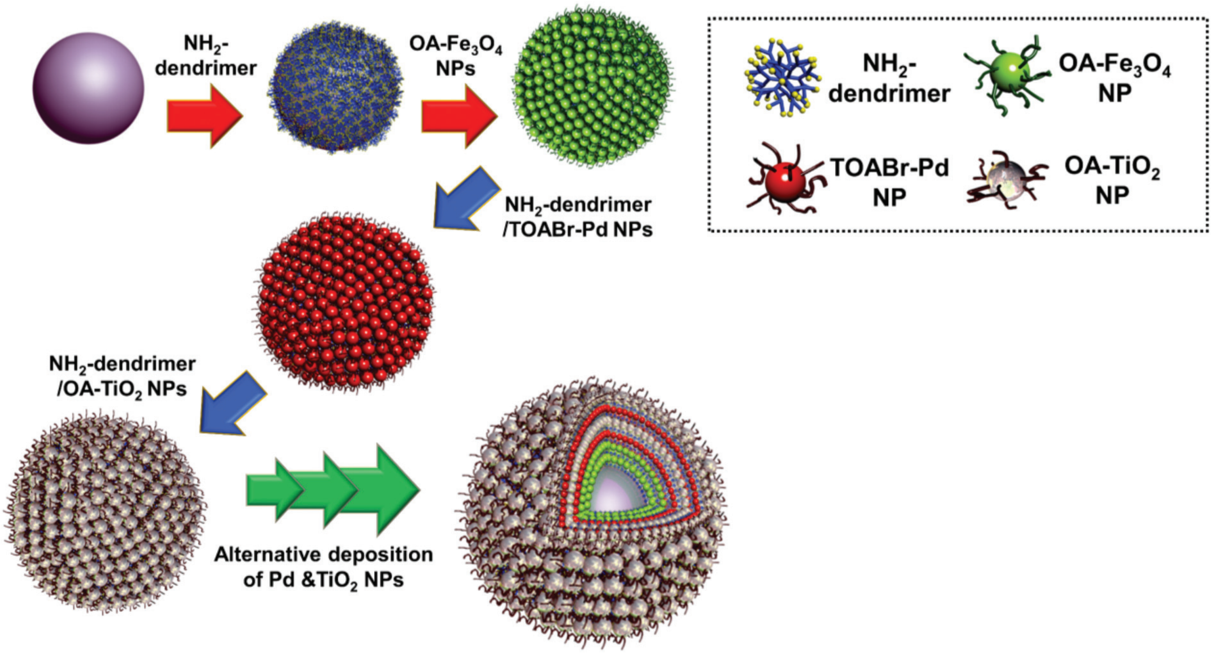

Scheme 1 Schematic for the preparation of recyclable multicatalytic colloids using ligand-exchange LbL assembly between a variety of hydrophobic metal (or metal oxide) NPs and NH_2–dendrimers.

Published on 19 October 2015. Downloaded by Korea University on 26/03/2016 04:39:26.

multicatalytic reactions of nanocomposite colloids depends strongly on the total loading amount of catalytic NPs inserted within multilayer shells. Other notable advantages of our approach are that these colloids can be easily collected for reuse, maintaining a high degree of catalytic properties even after repeated reaction. Furthermore, it should be noted that the type of outermost layer on recyclable multicatalytic colloids determines the stability of the colloidal dispersion in a variety of desired solvent media (*e.g.*, water, toluene, hexane, or triethylamine). These findings imply that the integrated properties (*i.e.*, the multicatalytic, magnetic, and high dispersion stability) of the respective functional NPs and NH_2–dendrimers are suitably manifested and improved by dense lateral and vertical packing of the constituent materials as well as by the number of deposited NP layers. Considering that a variety of well-defined catalytic NPs can be integrated into the multilayered shell, and furthermore that the resulting colloids are highly dispersible in various solvent media by LbL assembly, our strategy provides a basis for developing and designing high-performance recyclable multicatalytic colloids.

2. Experimental

2.1. Materials

Iron(III) acetylacetonate (Fe(acac)$_3$), 1,2-hexadecanediol, oleic acid (OA), oleylamine, benzyl ether, tetraoctylammonium bromide (TOABr), K_2PdCl_4, $NaBH_4$, titanium(IV) propoxide, *tert*-butylamine, 4-dimethylaminopyridine (DMAP), amine-functionalized poly(amidoamine) dendrimers (ethylenediamine core, generation 5.0) (*i.e.*, NH_2–dendrimers), polyethylenimine (PEI), 3,3′,5,5′-tetramethylbenzidine (TMB), phenylacetylene, iodobenzene, 4-iodoacetophenone, 1-iodo-4-nitrobenzene, triethylamine (TEA), and methylene blue (MB) were purchased from Sigma-Aldrich and used without purification. Silica colloids with a diameter of approximately 600 nm were purchased from Microparticles GmbH.

2.2. Preparation of samples

Synthesis of TOABr–Pd NPs. TOABr-stabilized Pd NPs with a diameter of approximately 2.6 nm were synthesized by a previously reported method.[38] A solution of 30 mM aqueous K_2PdCl_4 (30 mL) was added to 25 mM TOABr in toluene (80 mL). The transfer of the K_2PdCl_4 to the toluene phase could be clearly observed within a few seconds. A solution of 0.4 M $NaBH_4$ (25 mL) was added to the mixture. After 30 min, the separated aqueous phase was removed, and the toluene phase, containing the reduced TOABr–Pd NPs, was subsequently washed three times with 0.1 M H_2SO_4, 0.1 M NaOH, and H_2O.

Synthesis of cationic Pd NPs. An aqueous solution of 0.1 M DMAP (80 mL) was added to the as-prepared TOABr–Pd NP toluene solution (80 mL).[38] In this case, Pd NPs were directly phase-transferred from toluene to the aqueous phase within three hours, and the toluene phase was then removed. The resulting Pd NPs were stabilized by cationic DMAP ligands in the aqueous phase (*i.e.*, DMAP–Pd NPs).

Synthesis of OA–TiO_2 NPs. OA–TiO_2 NPs were prepared as reported elsewhere.[39] In a typical synthesis, 1.44 mL of *tert*-butylamine was dissolved in 14.3 mL of water, and the solution was transferred into a Teflon-lined stainless-steel autoclave. Subsequently, 0.21 g of titanium(IV) propoxide and 1.44 mL of OA were dissolved in 14.3 mL of toluene, and the solution was transferred into an autoclave without any stirring. The autoclave was sealed and maintained at 180 °C for 12 hours and then cooled to room temperature. The crude solution of OA–TiO_2 NPs was precipitated with methanol and further isolated by centrifugation. The purified OA–TiO_2 NPs were redispersed in toluene.

Synthesis of OA–Fe_3O_4 NPs. OA-stabilized Fe_3O_4 NPs of approximately 8 nm diameter were synthesized in toluene as previously reported by Sun *et al.*[37] Fe(acac)$_3$ (2 mmol), 1,2-hexadecanediol (10 mmol), OA (5 mmol), oleylamine (6 mmol), and benzyl ether (20 mL) were mixed and magnetically stirred under a nitrogen flow. The mixture was heated to 200 °C for two hours and heated to reflux (approximately 300 °C) for one hour under a nitrogen blanket. The black-colored mixture was cooled to room temperature by removing the heat source. Ethanol (40 mL) was added to the mixture under ambient conditions, and the black materials were precipitated and separated *via* centrifugation. These black products were dissolved in hexane in the presence of OA (0.05 mL) and oleylamine (0.05 mL). Centrifugation (6000 rpm, 10 min) was applied to remove any undispersed residue. A black-brown hexane dispersion of 8 nm OA–Fe_3O_4 NPs was produced.

Assembly of (NH_2–dendrimer/hydrophobic NP)$_n$ multilayers

(1) Flat substrate. A toluene solution of hydrophobic NPs stabilized by TOABr or OA ligands (*i.e.*, TOABr–Pd, OA–TiO_2, and OA–Fe_3O_4 NPs) and an ethanol solution of poly(amidoamine) dendrimers (NH_2–dendrimers) were prepared at concentrations of 10 and 1 mg mL^{-1}, respectively. For the LbL assembly of multilayers, silicon or quartz crystal microbalance (QCM) electrodes were irradiated with UV light ($\lambda \sim 350$ nm) for 10 min. The resulting negatively charged substrates were dipped into the NH_2–dendrimers for 30 min, washed twice with ethanol, and dried under a gentle nitrogen stream. The NH_2–dendrimer-coated substrates were dipped into a hydrophobic NP toluene (or other organic solution such as hexane or chloroform) solution for 30 min, followed by washing with the same solvent and thorough drying with nitrogen. After that, the substrates were dipped into the NH_2–dendrimer solution for 30 min again. These dipping cycles were repeated until the desired number of layers was obtained.

(2) Colloidal substrate. For the LbL assembly of multilayers onto colloidal substrates, 1 mL of a concentrated dispersion (5.0 wt%) of negatively charged 600 nm SiO_2 colloids was centrifuged at 3000 rpm for 5 min. After centrifugation, the supernatant was removed, and an NH_2–dendrimer solution of 1 mg mL^{-1} was added to the colloidal SiO_2 sediment followed by ultrasonication and a sufficient adsorption time. Excess NH_2–dendrimers were eliminated by two centrifugation (3000 rpm,

This journal is © The Royal Society of Chemistry 2016

Published on 19 October 2015. Downloaded by Korea University on 26/03/2016 04:39:26.

5 min)/wash cycles. To prepare multilayers on NH_2–dendrimer–silica colloids, a hydrophobic NP toluene solution with a concentration of 10 mg mL^{-1} was again added to the NH_2–dendrimer–silica colloids. The adsorption and washing cycles of hydrophobic NPs were the same as those used for the NH_2–dendrimers. It should be noted that the adsorption process of the functional components (*i.e.*, the NH_2–dendrimers and hydrophobic NPs) onto the colloidal substrates required no drying process. These processes were repeated until the desired layer number was deposited on the colloidal silica.

2.3. Characterization

High-resolution transmission electron microscopy (HR-TEM). The crystallinity and structure of the NPs (*i.e.*, TOABr–Pd and OA–TiO_2 NPs) and the recyclable multicatalytic SiO_2 colloids (*i.e.*, SiO_2/(NH_2–dendrimer/OA–Fe_3O_4 NP)$_3$/(NH_2–dendrimer/TOABr–Pd NP/NH_2–dendrimer/OA–TiO_2 NP)$_3$) were investigated by HR-TEM (Tecnai 20, FEI).

Scanning electron microscopy (SEM). The surfaces and diameters of the (NH_2–dendrimer/hydrophobic NPs)$_n$ multilayer-coated silica colloids were examined using SEM (Hitachi S-4800).

Fourier transform infrared spectroscopy (FTIR). Vibrational spectra were measured by FTIR spectroscopy (iS10 FT-IR, Thermo Fisher) in the attenuated total reflection (ATR) mode. The sample chamber was purged with nitrogen gas for two hours to eliminate water and CO_2 prior to conducting the FTIR measurement. An ATR-FTIR spectrum for the (NH_2–dendrimer/hydrophobic NP)$_n$ film deposited onto the Au-coated substrate was obtained from 256 scans with an incident angle of 80°. The acquired raw data were plotted after baseline correction, and the spectrum was smoothed using spectrum-analyzing software (OMNIC, Nicolet).

X-ray photoelectron spectroscopy (XPS). XPS spectra of the catalytic colloids with different bilayer numbers (*i.e.*, SiO_2/(NH_2–dendrimer/TOABr–Pd NP)$_{1,\ 3,\ \text{and}\ 5}$) were obtained using an AXIS-His spectrometer (KRATOS) with monochromatic Mg KR radiation (1253.6 eV). These survey spectra were recorded in the range of 0–1400 eV. The X-ray source was run at a reduced power of 150 W. The pressure in the analysis chamber was maintained at 5×10^{-9} Pa for measurement.

Quartz crystal microgravimetry (QCM) measurement. A QCM device (QCM200, SRS) was used to examine the mass of the deposited material after each adsorption step. The resonance frequency of the QCM electrodes was approximately 5 MHz. For preparing NH_2–dendrimer/TOABr–Pd NP multilayers on the QCM electrodes, an NH_2–dendrimer (or TOABr–Pd NP) layer was deposited onto the electrode, followed by two ethanol (or toluene) washes. The adsorbed mass of NH_2–dendrimers (or TOABr–Pd NPs), Δm, was calculated from the change in QCM frequency, ΔF, using the Sauerbrey equation:

$$\Delta F(\mathrm{Hz}) = -\frac{2{F_0}^2}{A\sqrt{\rho_q \mu_q}} \times \Delta m$$

here, F_0 (~ 5 MHz) is the fundamental resonance frequency of the crystal, A is the electrode area, and ρ_q (~2.65 g cm^{-3}) and μ_q (~2.95×10^{11} g cm^{-2} s^{-2}) are the density and shear modulus of quartz, respectively. This equation can be simplified as follows:

$$-\Delta F\ (\mathrm{Hz}) = 56.6 \times \Delta m_A$$

where Δm_A is the mass change per quartz crystal unit area in μg cm^{-2}. In this case, we measured the $-\Delta F$ per layer repeatedly (20 times) and calculated the resultant standard deviation of $-\Delta F$ for each layer.

Zeta potential measurement. Zeta potentials of the outermost-NH_2–dendrimer-coated colloids (*i.e.*, (SiO_2/(NH_2–dendrimer/TOABr–Pd NP)$_3$/NH_2–dendrimer) were measured using an electrophoretic light scattering spectrophotometer (Zeta-potential & Particle size Analyzer ELSZ, OTSUKA ELECTRONICS CO LTD)). The wavelength used was 633 nm with a scattering angle of 165°. All experiments were carried out at 20 °C.

Inductively coupled plasma-mass spectrometry (ICP-MS). The amount of Pd embedded within multicatalytic colloids (*i.e.*, SiO_2/(NH_2–dendrimer/OA–Fe_3O_4 NP)$_3$/(NH_2–dendrimer/TOABr–Pd NP/NH_2–dendrimer/OA–TiO_2 NP)$_3$) and the leaching amount of Pd in supernatant solution (*i.e.*, the solution that removes the (NH_2–dendrimer/TOABr–Pd NP)$_3$ multilayer-coated colloids in the reaction mixtures after the cycling test) were determined by ICP-MS (Elan DRC II, PerkinElmer).

X-Ray diffraction (XRD). The crystal structures of inorganic NPs (*i.e.*, OA–Fe_3O_4 NPs, TOABr–Pd NPs, and OA–TiO_2 NPs), which were coated onto the recyclable multicatalytic SiO_2 colloids, were characterized by XRD (Rigaku Model D/MAX-2500 V/PC). Data collection was performed over the 2θ range from 5 to 90° with Cu Kα radiation (λ = 1.54 Å).

2.4. Catalytic properties

TMB oxidation. Oxidation of 3,3′,5,5′-tetramethylbenzidine (TMB) was performed in 0.1 M NaOAc buffer solution (50 mL of pH 4.0) with 0.3 mM TMB and 100 mM H_2O_2 at 40 °C. The total amount of only Pd-coated colloid (*i.e.*, SiO_2/(NH_2–dendrimer/TOABr–Pd NP)$_n$) and magnetically retrievable multicatalytic colloids (*i.e.*, SiO_2/(NH_2–dendrimer/OA–Fe_3O_4 NP)$_3$/(NH_2–dendrimer/TOABr–Pd NP/NH_2–dendrimer/OA–TiO_2 NP)$_3$/NH_2–dendrimer) used for the TMB oxidation was fixed at 2.5 mg.

At given time intervals, 3 mL aliquots were collected from the solution. After the experiment, the catalytic colloids were removed by centrifugation or hand-held magnet, and the degree of TMB oxidation was analyzed by measuring the absorbance peak of TMB at 653 nm using UV-Vis spectroscopy (Lambda 35 UV-Vis spectrometer, PerkinElmer).

Sonogashira reaction. Pd-containing catalytic colloids (50 mg) were added to the 20 mL triethylamine (TEA) solution containing aryl iodide (4 mmol), phenylacetylene (5.2 mmol), and CuI (5 mol%). The reaction mixture was magnetically stirred under argon at 88 °C for the desired reaction time. After the reaction was completed, the product was analyzed by gas chromatography/mass spectrometry (GC/MS) using an external standard. For the GC/MS analysis, we used an Agilent GC/MS system consisting of an Agilent 6890 gas chromatograph and an Agilent 5973N mass spectrometer (Agilent, USA).

Published on 19 October 2015. Downloaded by Korea University on 26/03/2016 04:39:26.

Photocatalytic degradation of methylene blue. In a typical process, a 50 mL methylene blue (MB) aqueous solution (15 ppm) and the multifunctional colloids (35 mg) with photocatalytic activity (*i.e.*, $SiO_2/(NH_2$–dendrimer/OA–Fe_3O_4 NP$)_3$/(NH_2–dendrimer/TOABr–Pd NP/NH_2–dendrimer/OA–TiO_2 NP$)_3$/NH_2–dendrimer) were mixed in a 100 mL cylindrical quartz vessel. The photocatalytic reaction was induced by a 300 W xenon-mercury lamp placed at a distance of 10 cm (Newport, CA, USA). Prior to the reaction, the aqueous suspension including MB and the multicatalytic colloids was magnetically stirred in the dark for an hour to reach adsorption equilibrium. After the mixture was UV-irradiated at 365 nm, 3 mL aliquots were collected from the solution at given time intervals. Then, the photocatalytic colloids containing OA–Fe_3O_4 NPs were removed by a hand-held magnet, and the photodegradation results were analyzed by measuring the absorbance peak of MB at 665 nm using UV-Vis spectroscopy.

Cooperated multicatalytic reaction. Peroxidase-like activity (by Pd NPs) and photodegradation measurements (by TiO_2 NPs) were simultaneously performed in the same aqueous mixture containing multicatalytic colloids (*i.e.*, $SiO_2/(NH_2$–dendrimer/OA–Fe_3O_4 NP$)_3$/(NH_2–dendrimer/TOABr–Pd NP/NH_2–dendrimer/OA–TiO_2 NP$)_3$/NH_2–dendrimer). First, we prepared the mixture solution including MB (15 ppm) and 0.3 mM *o*-phenylenediamine (OPD) in the presence of 100 mM H_2O_2 at 40 °C. After that, multicatalytic colloids (12.5 mg) were added into the mixture solution, and then UV light (at 365 nm) was irradiated at a distance of 10 cm. In this case, the colloidal solution of 3 mL was collected every 5 min for investigating a degree of catalytic reaction, and successively the supernatant solution which removed the catalytic colloids, was also analyzed using UV-vis spectroscopy.

Recycling tests. The reusability of the magnetically responsive multicatalytic colloids was examined in both aqueous media (corresponding to TMB oxidation by Pd NP layers) and organic media (corresponding to the Sonogashira coupling reaction by Pd NP layers). These catalytic activities were measured after the addition of recyclable multicatalytic colloids in each cycle; these colloids were then magnetically separated by a hand-held magnet. The separated catalytic colloids were rinsed several times and used in the next cycle. Measurements for TMB oxidation and the Sonogashira reaction were conducted in the same manner.

3. Results and discussion

3.1. Adsorption behavior of LbL multilayers

The (NH_2–dendrimer/TOABr–Pd NP$)_n$ multilayer-coated catalytic colloids were prepared by LbL assembly in organic media. First, we prepared TOABr–Pd NPs with a diameter of approximately 2.6 nm in toluene (Fig. 1a and b),[38] and these NPs were directly deposited onto the NH_2–dendrimer-coated substrate. That is, when the TOABr–Pd NPs were deposited onto the NH_2–dendrimer-coated substrate, the TOABr (or OA) ligands loosely bound to the bottom surface of hydrophobic NPs were easily replaced by the NH_2 moieties of dendrimer due to the higher affinity between $-NH_2$ groups of dendrimers and the surface of Pd NPs (see the ESI, Fig. S1a†). Although the outermost surface of Pd NPs was still stabilized with the hydrophobic TOABr ligands, these ligands were successively replaced by the NH_2–dendrimer in the next deposition step. This ligand exchange process was monitored by Fourier transform infrared spectroscopy (FTIR) in the attenuated total reflection (ATR) mode to understand the adsorption mechanism governing the accumulation of LbL-assembled NH_2–dendrimer/TOABr–Pd NP multilayers (Fig. 1c and d). The resultant film (*i.e.*, SiO_2 substrate/NH_2–dendrimer/TOABr–Pd NP) exhibited C–H stretching peaks (at 2952, 2927, and 2850 cm^{-1}) originating from long alkyl chains of TOABr ligands and N–H scissor bending peaks (at 1550–1640 cm^{-1}) from the primary amine groups of NH_2–dendrimers (see ESI, Fig. S1b†). Additionally, these N–H scissor bending peaks were overlapped with the C=O stretching peak from amide groups of dendrimers in the range of 1550 and 1640 cm^{-1}.[40]

However, further adsorption of NH_2–dendrimers onto the outermost TOABr–Pd NP-coated substrate almost completely eliminated the C–H stretching peaks confirming the presence of TOABr ligands through observation of the FTIR spectra. In contrast, the N–H bending peaks arising from the NH_2 groups of dendrimers intensified, as shown in Fig. 1c. These findings imply that the TOABr ligands bound to the surface of Pd NPs are successfully replaced by the NH_2 groups of dendrimers because of their higher affinity for Pd NPs during deposition, and additionally, that the presence of TOABr ligands can be observed in only the outermost TOABr–Pd NP layer of (NH_2–dendrimer/TOABr–Pd NP$)_n$ multilayers. That is, the top surface of the TOABr–Pd NP layer unbound to the NH_2–dendrimer layer is still stabilized with the remaining TOABr ligands. As a result, the C–H stretching peaks periodically appear and disappear with increasing bilayer number from 0.5 (*i.e.*, substrate/NH_2–dendrimer) to 3.0 (*i.e.*, substrate/(NH_2–dendrimer/TOABr–Pd NP$)_3$) (Fig. 1c). A time-dependent FTIR analysis of adsorption also showed that the ligand-exchange reaction between the TOABr ligands and the NH_2 groups of the dendrimers is nearly completed in approximately 30 min, and that the surface of the resultant Pd NP layer is restabilized by the NH_2 groups of the dendrimers *via* a coordination bond (Fig. 1d). It has been reported that in the case of hydrophobic Au NPs stabilized by TOABr ligands, the bromide ion (Br^-) is directly associated with the surface of the Au NPs and that TOA^+ ions are required to preserve electroneutrality in the TOABr–Au NPs as a whole.[41] Therefore, these TOABr ligands loosely bound to the metal surface can be easily replaced by the primary amine-functionalized ligands with a higher affinity for the metal NPs.[41,42]

Based on these results, the (NH_2–dendrimer/TOABr–Pd NP$)_n$ multilayers were deposited onto the SiO_2 colloids with a diameter of 600 ± 5 nm, using alternating deposition of NH_2–dendrimers in ethanol and TOABr–Pd NP in toluene. As shown in Fig. 2a–d, as the bilayer number (*n*) increased from 0 to 9, the diameter of the multilayer-coated colloids increased from

This journal is © The Royal Society of Chemistry 2016

Published on 19 October 2015. Downloaded by Korea University on 26/03/2016 04:39:26.

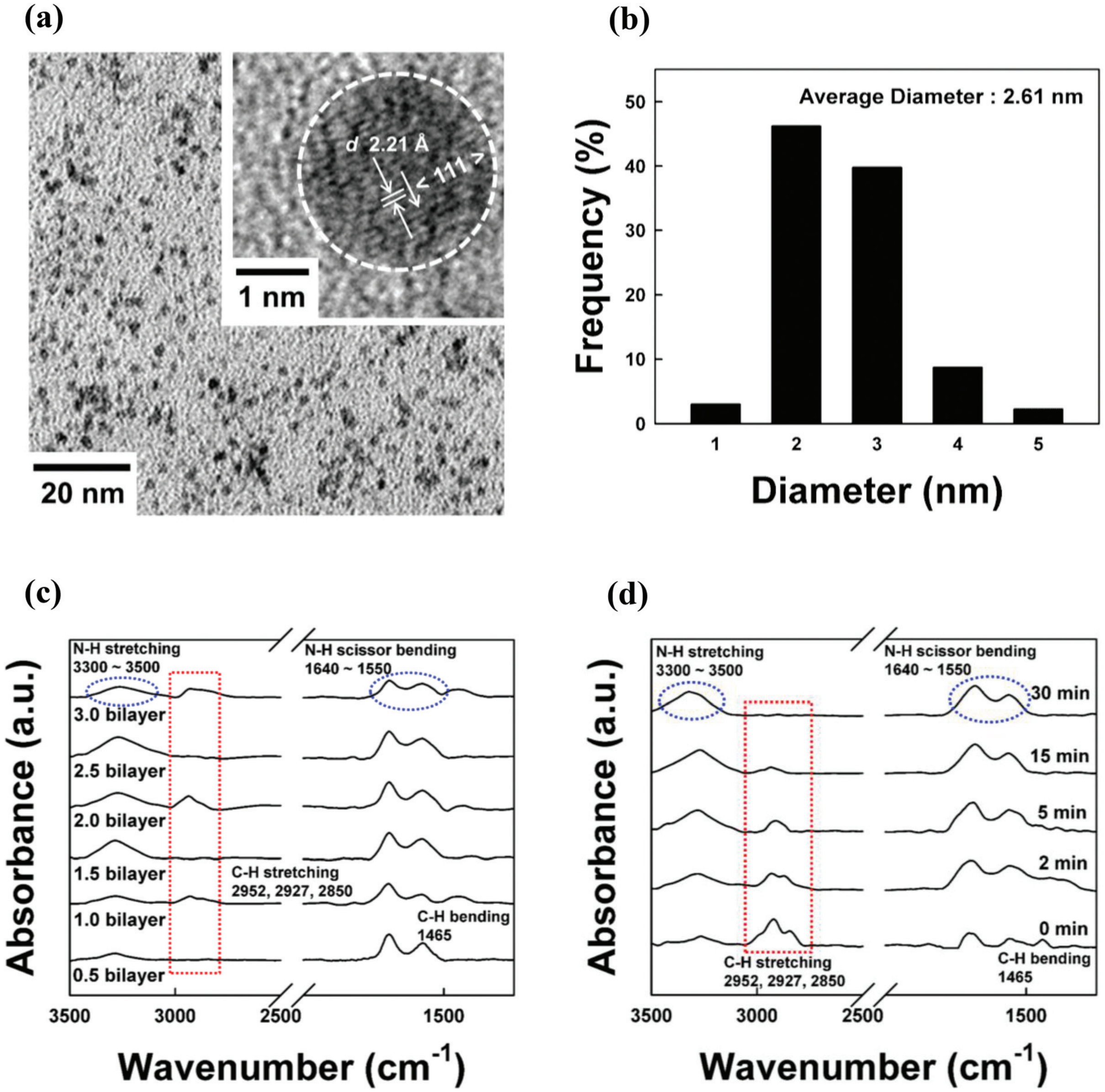

Fig. 1 (a) High-resolution transmission electron microscopy (HR-TEM) image of TOABr–Pd NPs with a diameter of approximately 2.6 nm. (b) Size-distribution histogram of TOABr–Pd NPs measured from HR-TEM images. (c) ATR-FTIR spectra of $(NH_2$–dendrimer/TOABr–Pd NP$)_n$ multilayer films as a function of bilayer number (n). (d) ATR-FTIR spectra of substrate/$(NH_2$–dendrimer/TOABr–Pd NP$)_1$/outermost NH_2–dendrimer film with increasing deposition time of the outermost NH_2–dendrimer layer from 0 to 30 min.

approximately 600 to 708 nm without colloidal aggregation. This well-organized structure of multilayer-coated colloids was also confirmed by the X-ray photoelectron spectroscopy (XPS) analysis (see the ESI, Fig. S2†). Although the Pd composition measured from 1 bilayer-coated colloids was rather lower than that of other bilayer number-coated colloids, this result was due to the insufficient coverage of first NH_2–dendrimer layer adsorbed onto SiO_2 colloids.

In contrast, when linear-type NH_2-functionalized polymers with low molecular weight, such as poly(ethylene imine) (PEI, MW ~ 800 and 25 000), were used instead of NH_2–dendrimers, the (PEI/TOABr–Pd NPs$)_n$ multilayer-coated colloids were detectably aggregated after the deposition of only five bilayers. These findings can be attributed to a bridging effect between linear-type neutralized polymers adsorbed simultaneously onto adjacent colloids (see the ESI, Fig. S3†). Therefore, the homogeneous and uniform coating shown in the $(NH_2$–dendrimer/TOABr–Pd NP$)_n$ multilayer-coated colloids can be attributed to the globular and spherical shape of the NH_2–dendrimers and NPs, respectively. Furthermore, in the case of electrostatic LbL assembly between cationic Pd NPs and anionic polyelectrolytes, it should be noted that the total thickness of the assembled multilayers was much less than that of $(NH_2$–dendrimer/TOABr–Pd NPs$)_n$ multilayer-coated colloids,

Published on 19 October 2015. Downloaded by Korea University on 26/03/2016 04:39:26.

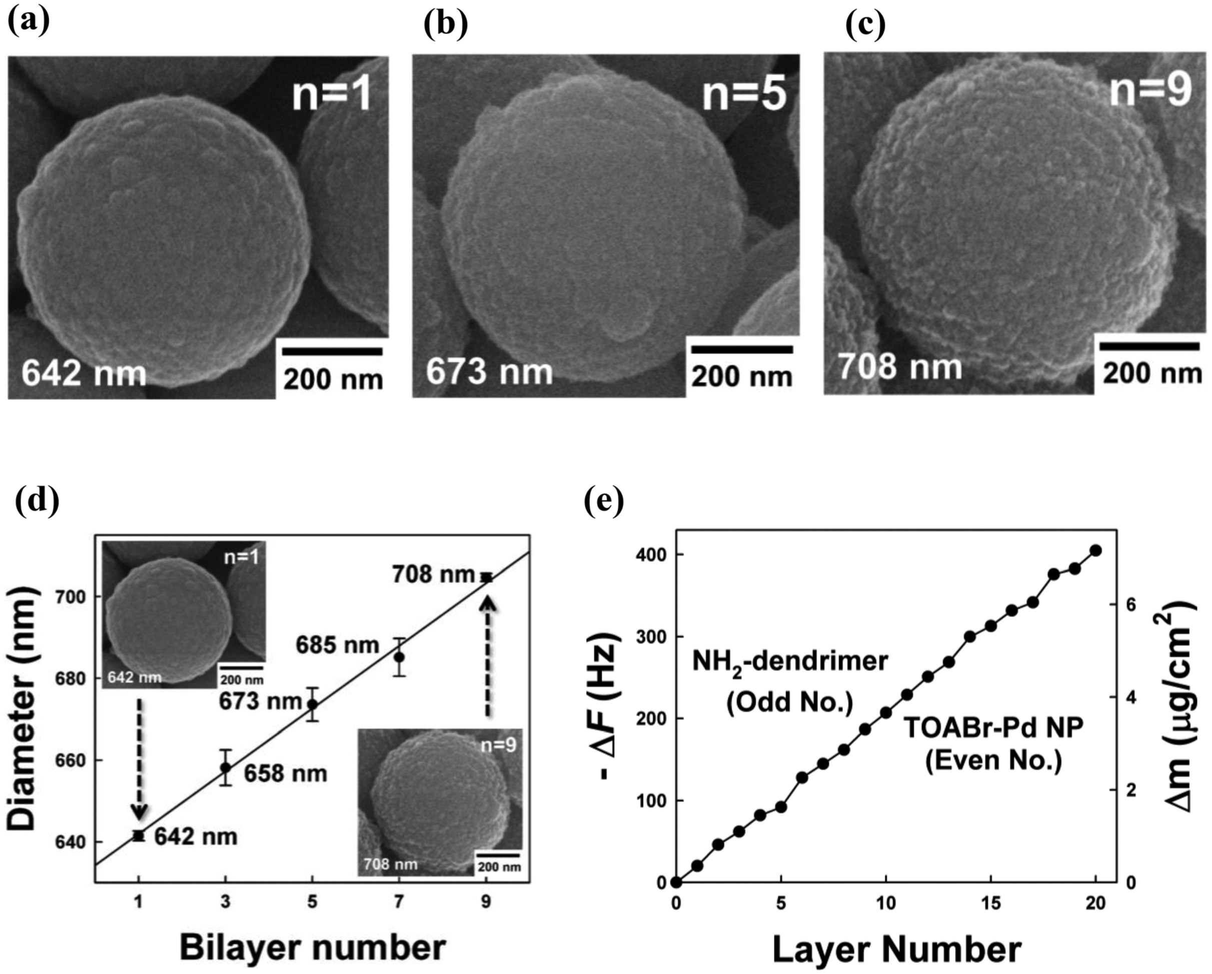

Fig. 2 Scanning electron microscopy (SEM) images of (NH_2–dendrimer/TOABr–Pd NP)$_n$ multilayer-coated SiO_2 colloids with (a) $n = 1$, (b) $n = 5$, and (c) $n = 9$. (d) Size change of (NH_2–dendrimer/TOABr–Pd NP)$_n$ multilayer-coated SiO_2 colloids with increasing bilayer number (n). The insets show SEM images of (NH_2–dendrimer/TOABr–Pd NP)$_n$ multilayer-coated SiO_2 colloids (n = 1 and 9). (e) QCM data for the (NH_2–dendrimer/TOABr–Pd NP)$_n$ as a function of layer number.

as a result of the strong electrostatic repulsion occurring among the cationic Pd NPs (see the ESI, Fig. S4†).

Although we could not precisely measure the amount of adsorbed Pd NP on the SiO_2 colloidal substrate, quantitative analysis of (NH_2–dendrimer/TOABr–Pd NP)$_n$ multilayers using a quartz-crystal microbalance (QCM) with a flat electrode allowed us to estimate the amount of TOABr–Pd NPs adsorbed onto 600 nm silica colloids with a surface area of 1.16×10^{-8} cm^2 (Fig. 2e). In this case, the average mass of TOABr–Pd NPs adsorbed per unit area was calculated to be approximately 493 ng cm^{-2}. However, this average mass value included the mass of the bulky TOABr ligands ($M_w \sim 546.8$ g mol^{-1}) bound to the outermost Pd NP layer. Therefore, for a more exact analysis on the adsorbed amount of Pd NPs buried within multilayers, the outermost TOABr ligands were replaced by primary amine-functionalized ethylene diamine (EDA) with a small molecular weight (M_w) of 60.1 g mol^{-1} and a boiling point temperature of 116 °C. In this case, the remaining TOABr ligands could be completely removed after the additional ligand exchange reaction (see the ESI, Fig. S5†). That is, when EDA was deposited onto the electrode/NH_2–dendrimer/TOABr–Pd NP, and furthermore this multilayer-coated electrode was dried above 150 °C, the adsorbed mass of TOABr–Pd NPs changed from 493 to 232 ng cm^{-2}. These results implied that the mass of remaining TOABr ligands was approximately 261 ng cm^{-2} (The mass change, Δm, of the Pd NPs was calculated from the frequency change, ΔF, of the QCM. A more detailed calculation is shown in the Experimental section). Considering that the mass density of Pd is 12.02 g cm^{-3} and the volume of the Pd NPs with a diameter of 2.61 nm was 9.31×10^{-21} cm^3, the mass of a single Pd NP was approximately 1.12×10^{-10} ng. Therefore, the number and mass of NPs in a single layer adsorbed per silica colloid was approximately 2.403×10^4 NPs, and 2.69×10^{-15} g, respectively.

Additionally, the dispersion stability of (NH_2–dendrimer/TOABr–Pd NP)$_n$ multilayer-coated colloids in various solvent

Published on 19 October 2015. Downloaded by Korea University on 26/03/2016 04:39:26.

media strongly depends on the hydrophobicity/hydrophilicity of the outermost layer. That is, when the outermost layer of a nanocomposite colloid is coated by TOABr–Pd NPs that can be well-dispersed in various organic media (*e.g.*, chloroform, toluene, and hexane), the multilayer-coated colloids (*i.e.*, SiO_2/(NH_2–dendrimer/TOABr–Pd NP$)_3$) themselves exhibit a high degree of dispersion stability in these organic media (Fig. 3a). However, when the outermost layer is coated by NH_2–dendrimers, the multilayer-coated colloids (*i.e.*, (SiO_2/(NH_2–dendrimer/TOABr–Pd NP$)_3$/NH_2–dendrimer)) can only be dispersed well in water and ethanol (Fig. 3b). In particular, when the outermost NH_2–dendrimer-coated colloids are dispersed in aqueous media, the NH_2–dendrimers become positively charged because of the partial conversion from uncharged amine groups to cationic amine groups in deionized water at pH 5.8. Choi and Rubner reported that the pK_a value (*i.e.*, the pH value at which 50% of the functional groups of a polymer are ionized) of an amine-functionalized polymer, such as poly(allylamine hydrochloride) (PAH), is approximately 9.0.[43] Therefore, the protonation of the NH_2–dendrimers in water at pH 5.8 can enable electrostatically charged colloids to be highly miscible in aqueous media without any colloidal aggregation because of electrostatic repulsion among like-charged colloids. In this case, the zeta potential of the outermost NH_2–dendrimer-coated colloids (*i.e.*, SiO_2/(NH_2–dendrimer/TOABr–Pd NP$)_3$/NH_2–dendrimer) was measured to be approximately 31.0 ± 2.0 mV. Based on these results, in the case of dispersing the outermost TOABr–Pd NP-coated and the outermost NH_2–dendrimer-coated colloids in a mixed solvent (*i.e.*, a mixture containing toluene, water, and chloroform), the hydrophobic colloids can be dispersed in the upper (toluene) and lower (chloroform) solvent media (sample A of Fig. 3c), whereas hydrophilic colloids were only dispersed in the intermediate water solvent (sample B of Fig. 3c). This high dispersion stability of the (NH_2–dendrimer/TOABr–Pd NP$)_n$ multilayer-coated colloids in various solvent media is particularly important in catalysis because colloidal agglomeration significantly reduces the catalytic surface area and thus the catalytic activity.

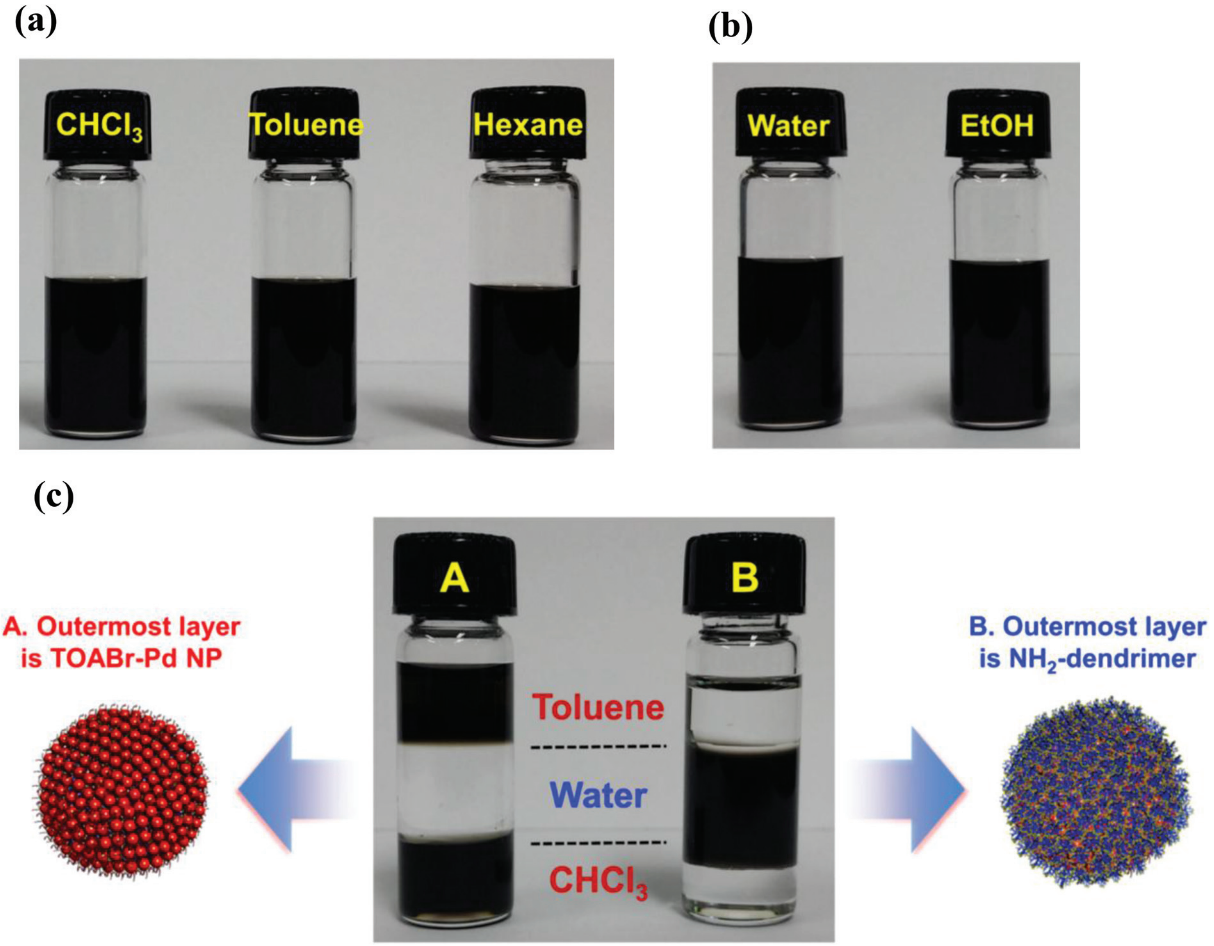

Fig. 3 (a) The outermost TOABr–Pd NP-coated SiO_2 colloids dispersed in chloroform, toluene, hexane, and triethylamine (TEA). (b) The outermost NH_2–dendrimer-coated SiO_2 colloids dispersed in water and ethanol. (c) Colloidal dispersion depending on the surface wettability of the outermost layer in a mixed solvent (*i.e.*, toluene, water, and chloroform).

Published on 19 October 2015. Downloaded by Korea University on 26/03/2016 04:39:26.

3.2. TMB oxidation of $(NH_2$–dendrimer/TOABr–Pd NP$)_n$ multilayer-coated colloids

To confirm the catalytic activity of Pd NP multilayer-coated colloids with an outermost NH_2–dendrimer layer in aqueous media, we examined the oxidation of 3,3′,5,5′-tetramethylbenzidine (TMB).[44,45] In general, the ability to catalyze the oxidation of organic substrates to decrease their toxicity and/or activate a color change is used in waste water treatment and/or as a detection tool.[44] Fig. 4a shows the UV-vis spectra of three different buffer solutions containing 0.1 M NaOAc at pH 4.0 with the addition of (i) 0.3×10^{-3} M TMB alone; (ii) 0.3×10^{-3} M TMB and 0.1 M H_2O_2; (iii) 0.3×10^{-3} M TMB, 0.1 M H_2O_2, and $(NH_2$–dendrimer/TOABr–Pd NP$)_{3.5}$ multilayer-coated SiO_2 colloids at 40 °C.[44,45] In this experiment, the solutions without catalytic colloids displayed no absorbance peaks in the measured wavelength range. In contrast, when the catalytic colloids were added to the TMB solution with H_2O_2, the catalytic colloidal solution exhibited intense characteristic absorbance peaks (at 370 and 653 nm) in the UV-Vis spectrum, followed by a blue color. These absorption bands of the TMB solution are attributed to the charge-transfer complexes derived from the one-electron oxidation of TMB, followed by a distinct blue color with characteristic UV-Vis absorbance

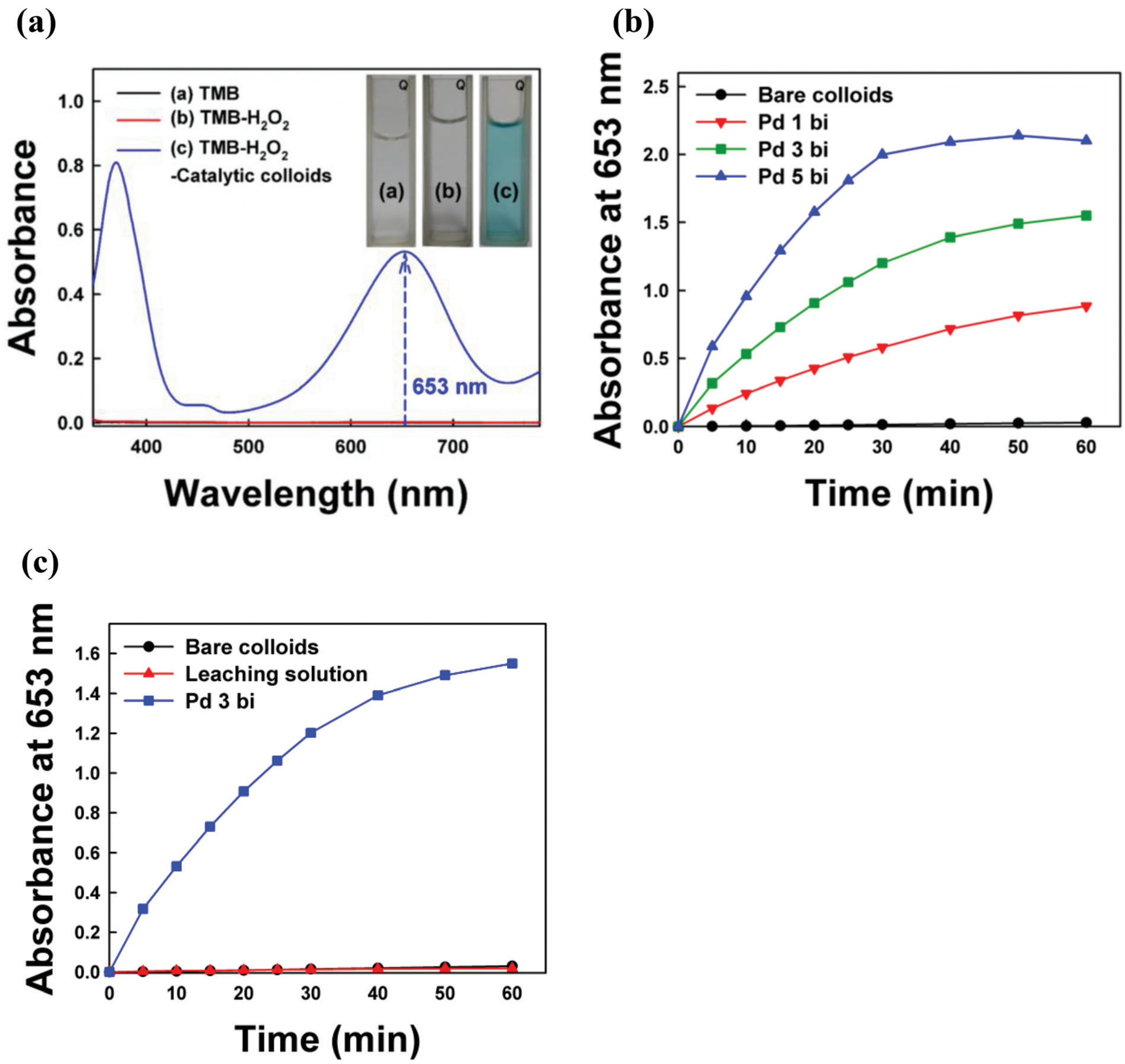

Fig. 4 (a) UV-Vis spectra of 0.1 M NaOAc buffer solutions (pH 4.0) containing (i) 0.3×10^{-3} M TMB alone; (ii) 0.3×10^{-3} M TMB and 0.1 M H_2O_2; and (iii) 0.3×10^{-3} M TMB, 0.1 M H_2O_2 and $(NH_2$–dendrimer/TOABr–Pd NP$)_{3.5}$ multilayer-coated SiO_2 colloids at 40 °C for 10 min. The inset shows the color change resulting from the oxidation reaction of TMB. (b) Time-dependent absorbance changes of the TMB-oxidation system at 653 nm in the presence of $(NH_2$–dendrimer/TOABr–Pd NP$)_n$ multilayer-coated SiO_2 colloids (n = 0, 1.5, 3.5, and 5.5). (c) Time-dependent absorbance evolution of the TMB-oxidation system at 653 nm using the leaching solution.

This journal is © The Royal Society of Chemistry 2016

Published on 19 October 2015. Downloaded by Korea University on 26/03/2016 04:39:26.

peaks at 370 and 653 nm.[46] Therefore, our results demonstrate that the Pd NP multilayer-coated colloids decompose H_2O_2 into hydroxyl radicals ($OH^•$), which can oxidize TMB substrates.[45]

Based on these results, we further investigated the TMB-oxidation reaction of colloids as a function of the number of layers of inserted Pd NPs (*i.e.*, SiO_2/(NH_2–dendrimer/TOABr–Pd NP)$_{n=0,1.5,\ 3.5,\ \text{and}\ 5.5}$). As shown in Fig. 4b, the absorbance intensity measured at 653 nm was rapidly and significantly increased with increasing bilayer number from 0 to 5.5. For example, the absorbance intensity of the (NH_2–dendrimer/TOABr–Pd NP)$_{5.5}$-coated colloidal solution, which had nearly stabilized after 30 min, was approximately 3.5 times higher than that of the (NH_2–dendrimer/TOABr–Pd NP)$_{1.5}$-coated colloidal solution (which exhibited a slower oxidation reaction over the same time). These findings imply that an increase in the adsorbed amount of Pd NPs induces a faster and a stronger catalytic reaction, and consequently, the catalytic ability of LbL-assembled colloids can be easily but precisely manipulated by adjusting the number of deposited Pd NP layers. We also highlight the finding that catalytic colloids prepared from LbL assembly are stable as a result of coordination bonding between the NH_2–dendrimers (with multiple binding sites) and the Pd NPs. That is, we rule out the possibility that the TMB oxidation shown in our study can be caused by Pd NPs leached from multilayer-coated colloids. To demonstrate multilayer robustness, the catalytic colloids were incubated under the same reaction conditions (*i.e.*, pH 4.0 and 40 °C) for three hours and were then precipitated by centrifugation. After the thorough removal of catalytic colloids in solution, we investigated the TMB-oxidation reaction in the supernatant (or leaching) solution. As shown in Fig. 4c, the absorbance intensity originating from TMB oxidation in the supernatant solution was negligible, which is the same result obtained from the pristine solution containing no catalytic colloids. More specifically, when the leaching amount of Pd NPs was investigated using inductively coupled plasma-mass spectrometry (ICP-MS), the Pd NPs of 0.96 ppm were detected in the supernatant solution. These results strongly support our assertion that catalytic Pd NPs were not detached from the multilayer-coated colloids, and therefore, the catalytic reactions shown in Fig. 4a and b originated not from detached Pd NPs but entirely from (NH_2–dendrimer/TOABr–Pd NP)$_n$-coated colloids. Additionally, the extremely low leaching amount of Pd NPs implies that the catalytic colloids prepared from our approach are highly stable in reaction media. To our knowledge, our approach of using (NH_2–dendrimer/catalytic NP)$_n$ multilayers for the preparation of catalytic colloids has not been previously reported. Although Niu *et al.* reported that Pd NPs inserted within the interiors of hydroxyl (OH)-terminated dendrimers could be used as a catalyst for the hydrogenation reaction of olefins,[47] their approach differs from ours in that the exteriors (*i.e.*, NH_2 moieties) of the NH_2–dendrimers are LbL-assembled with TOABr–Pd NPs *via* ligand-exchange reactions in our work, and additionally, these LbL multilayers are formed around colloidal substrates.

3.3. Sonogashira reaction of (NH_2–dendrimer/TOABr–Pd NP)$_n$ multilayer-coated colloids

As mentioned earlier, the (NH_2–dendrimer/TOABr–Pd NP)$_3$ multilayer-coated colloids with outermost TOABr–Pd NP layers were dispersed well in a variety of organic media, such as toluene, hexane, chloroform or triethylamine. To evaluate the catalytic ability of the LbL-assembled multilayer-coated colloids in nonpolar media, and demonstrate the effectiveness of our approach, we performed a Pd-catalyzed Sonogashira reaction,[5,48] which forms a carbon–carbon bond between aryl (or vinyl) halide and terminal alkynes in the presence of palladium and copper catalysts (Scheme 2). It is well known that the Sonogashira coupling reaction is very effective in preparing arylalkynes and conjugated enynes that are used as precursors for pharmaceuticals, natural products, and organic materials.[48] For example, Pedersen *et al.* reported that ellipticine (with anticancer properties) could be synthesized from ethyl 2-(4-pyridyl)acetate through the Sonogashira coupling reaction.[49] Based on this well-known reaction system, we tried to demonstrate the effectiveness of our approach.

For the current investigation, phenylacetylene as a terminal alkyne was reacted with various types of aryl iodide in two different types of copper catalyst (CuI)-inserted triethylamine (TEA) media with and without the (NH_2–dendrimer/TOABr–Pd NP)$_3$ multilayer-coated colloids (Table 1).[48] In this case, triethylamine (TEA) media with tertiary amine had no affinity with TOABr–Pd NPs, which was confirmed by FTIR spectroscopy (see the ESI, Fig. S6†).

As shown in Table 1, when the Pd NP multilayer-coated colloids were added to the reaction mixture (entries 2, 4, and 6 of Table 1), the yield of the desired products dramatically increased compared to that of the copper-catalyst-containing mixture without the Pd NP multilayer-coated colloids (entries 1, 3, and 5 of Table 1). For example, when iodobenzene was introduced into the reaction system with only the copper catalyst, the yield of the coupling product (*i.e.*, diphenylacetylene) was measured to be approximately 17% (entry 1 of Table 1). However, in the presence of Pd NP multilayer-based colloids and CuI, the product yield was as high as 98% for the same reaction time (entry 2 of Table 1). Additionally, when we investigated the possibility of Cu incorporation into Pd NP multilayer-coated colloids after the Sonogashira reaction using the energy dispersive spectrometer (EDS), we did not observe the presence of any Cu within the colloids (data not shown). These results indicate that Pd NP multilayer-based colloids can be successfully used as catalytic colloids in organic media as well as in aqueous media. Additionally, given that a variety of well-defined NPs with desired functionalities (particularly, magnetic and other catalytic properties) can be easily incorporated into multilayers using ligand-exchange LbL assembly, our approach provides a route for designing catalytic colloids with more integrated functionalities.

Published on 19 October 2015. Downloaded by Korea University on 26/03/2016 04:39:26.

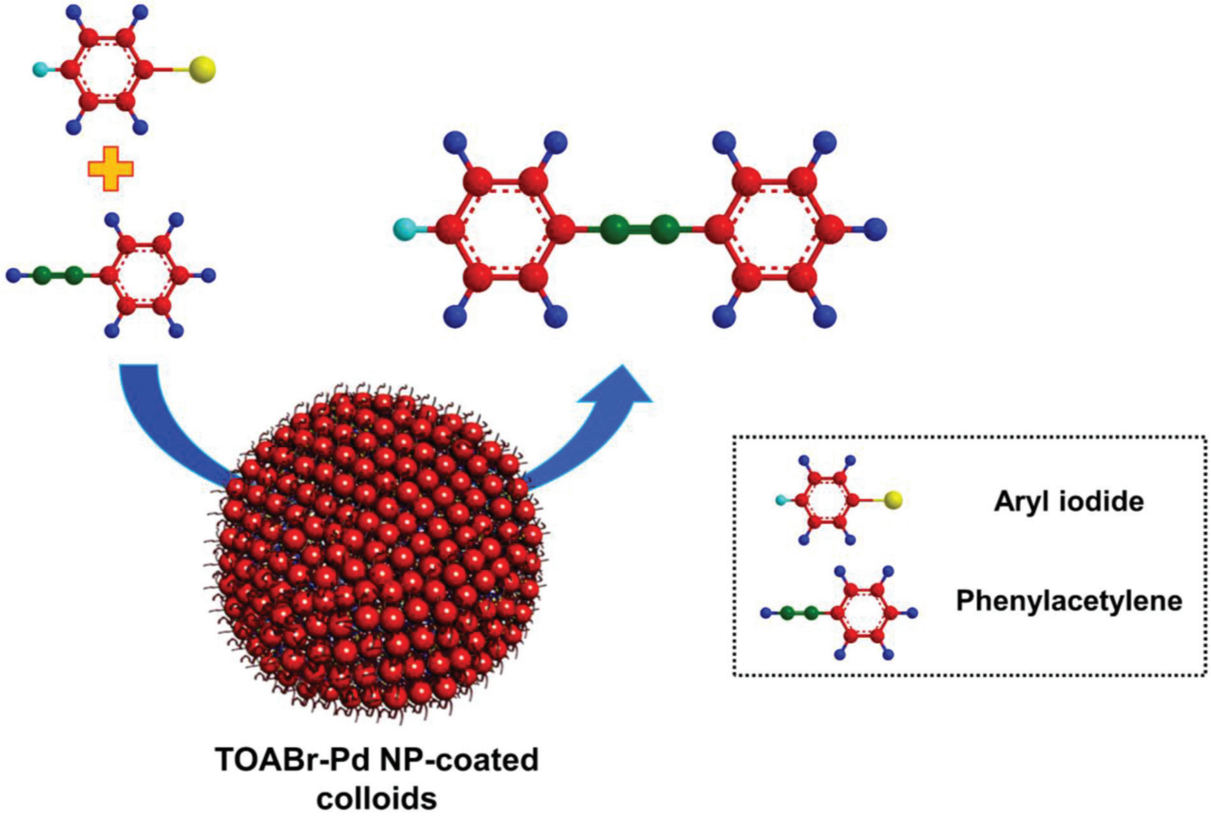

Scheme 2 Sonogashira coupling reaction between aryl iodide and phenylacetylene using (NH$_2$–dendrimer/TOABr–Pd NP)$_3$ multilayer-coated colloids.

Table 1 Sonogashira coupling reaction of aryl iodide using (NH$_2$–dendrimer/TOABr–Pd NP)$_3$ multilayer-coated colloids[a]

Entry	Substrate (Ar–I)	Terminal alkyne (phenylacetylene)	Coupling product	Yield[b] [%]
1[c]	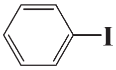	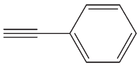	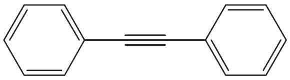	17
2	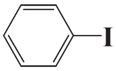	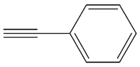	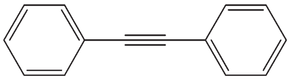	98
3[c]	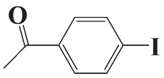	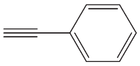	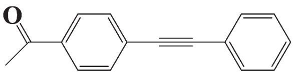	1.3
4	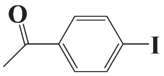	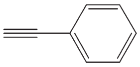	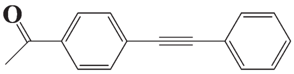	85
5[c]	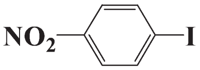	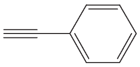	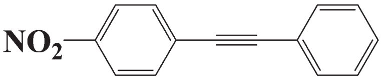	46
6	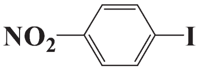	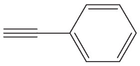	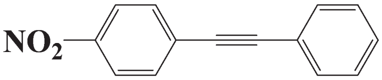	99

[a] Reaction conditions: Ar–I (4 mmol), phenylacetylene (5.2 mmol), CuI (5.0 mol%), (NH$_2$–dendrimer/TOABr–Pd NP)$_3$ multilayer-coated colloids (50 mg), and TEA (20 mL) at 88 °C under argon. [b] Yields determined by GC-MS analysis. [c] Without catalysts to compare with the catalytic ability of Pd-coated colloids.

This journal is © The Royal Society of Chemistry 2016

Published on 19 October 2015. Downloaded by Korea University on 26/03/2016 04:39:26.

3.4. Multicatalytic reactions of nanocomposite colloids with OA–Fe_3O_4, TOABr–Pd, and OA–TiO_2 NPs

To demonstrate a more challenging possibility, magnetic OA–Fe_3O_4 NPs and photocatalytic OA–TiO_2 NPs as well as TOABr–Pd NPs were incorporated into functional multilayers for the preparation of magnetically retrievable colloids. In our previous study, it was reported that OA–Fe_3O_4 NPs, similar to TOABr–Pd NPs, could be directly LbL-assembled with NH_2-functionalized polymers *via* ligand exchange between the OA groups loosely bound to the Fe_3O_4 NPs and the NH_2 groups of polymers.[36] We also observed that OA–TiO_2 NPs with a diameter of approximately 12.8 nm, which can be used as photocatalytic NPs,[39,50] could be adsorbed onto a NH_2–dendrimer-coated substrate (see the ESI, Fig. S7c and S7d†).

Based on these results, 8 nm OA–Fe_3O_4, 12.8 nm OA–TiO_2 NPs, and 2.6 nm TOABr–Pd NPs were integrated into the multilayer shell of SiO_2 colloids (*i.e.*, SiO_2/(NH_2–dendrimer/OA–Fe_3O_4 NP)$_3$/(NH_2–dendrimer/TOABr–Pd NP/NH_2–dendrimer/OA–TiO_2 NP)$_3$), as displayed in the HR-TEM image shown in Fig. 5a. The respective crystalline phases of the inorganic NPs (*i.e.*, OA–Fe_3O_4 NP, TOABr–Pd NP, and OA–TiO_2 NP) embedded within multilayer-coated colloids were identified by X-ray diffraction (XRD) (Fig. 5b).[33,51,52] The measured film thickness of

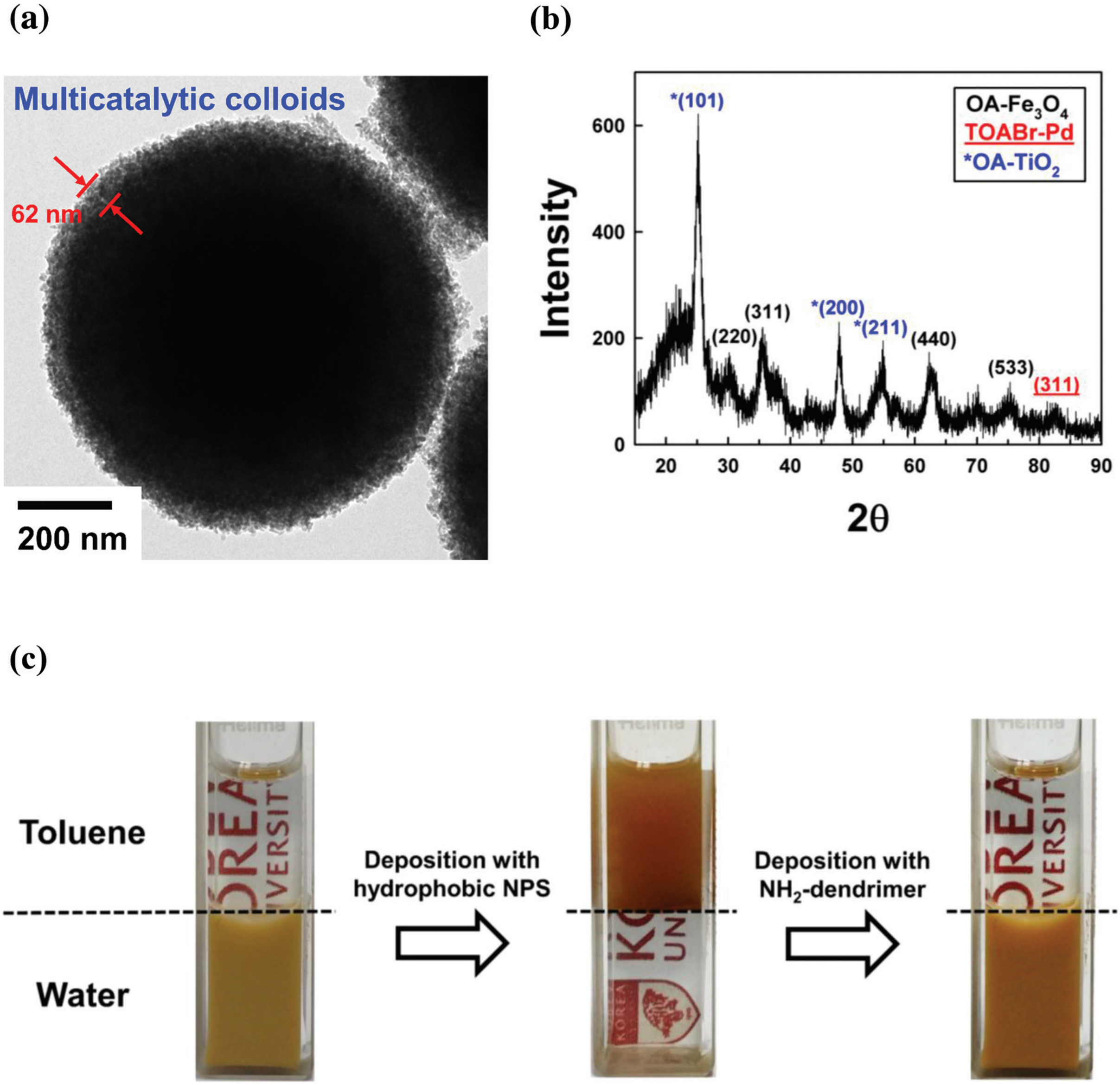

Fig. 5 (a) HR-TEM image and (b) XRD pattern of the multicatalytic colloids. Here, the structure of the multicatalytic colloids was SiO_2/(NH_2–dendrimer/OA–Fe_3O_4 NP)$_3$/(NH_2–dendrimer/TOABr–Pd NP/NH_2–dendrimer/OA–TiO_2 NP)$_3$. (c) Reversible phase transfer of the multicatalytic colloids between water and toluene according to the type of the outermost layer. The deposition of NH_2–dendrimers and hydrophobic NPs (*i.e.*, OA–Fe_3O_4, TOABr–Pd, or OA–TiO_2 NP) as an outermost layer causes the colloids to be dispersed well in water and toluene, respectively.

Published on 19 October 2015. Downloaded by Korea University on 26/03/2016 04:39:26.

62 nm was less than the ideal film thickness of approximately 77.7 nm (calculated from 8 nm OA–Fe_3O_4, 12.8 nm OA–TiO_2, 2.6 nm TOABr–Pd, and the NH_2–dendrimer layer thickness of approximately 1 nm), which was caused by the insufficient packing density of adsorbed NPs. However, it should be noted again that this thickness could not be easily obtained from electrostatic LbL assembly (see the ESI, Fig. S4b†).

As mentioned earlier, when the outermost NH_2–dendrimer-coated colloids were dispersed in water at pH 10, the outermost dendrimer layers still carried a large number of uncharged amine groups,[43] which could induce the deposition of hydrophobic NPs, such as OA–Fe_3O_4, OA–TiO_2, and TOABr–Pd NPs, without the additional insertion of an alcohol-soluble hydrogen-bonding polymer layer. As a result, the alternating deposition of the NH_2–dendrimers and hydrophobic NPs could allow the multilayer-coated colloids (*i.e.*, SiO_2/(NH_2–dendrimer/OA–Fe_3O_4 NP)$_3$/(NH_2–dendrimer/TOABr–Pd NP/NH_2–dendrimer/OA–TiO_2 NP)$_3$) to be reversibly phase-transferred between aqueous and nonpolar media (Fig. 5c), which exactly coincides with the solvent-dispersion behavior of (NH_2–dendrimers/TOABr–Pd NP)$_n$-coated colloids shown in Fig. 3.

On the basis of these results, we demonstrated that three different types of catalytic reactions (namely, TMB oxidation, photocatalytic degradation of methylene blue (MB), and Sonogashira reactions) can be induced by multicatalytic colloids incorporating OA–Fe_3O_4, TOABr–Pd, and OA–TiO_2 NPs. First, we tested the TMB oxidation (by TOABr–Pd NPs) of multicatalytic colloids with an outermost NH_2–dendrimer layer (*i.e.*, SiO_2/(NH_2–dendrimer/OA–Fe_3O_4 NP)$_3$/(NH_2–dendrimer/TOABr–Pd NP/NH_2–dendrimer/OA–TiO_2 NP)$_3$/NH_2–dendrimer) in aqueous solution. As shown in Fig. 6a, the absorbance intensity (at 653 nm) of the multicatalytic colloidal solution, a surrogate measure of TMB oxidation, significantly increased with increasing reaction time. The degree of TMB oxidation obtained from multicatalytic colloids was similar to that of the SiO_2/(NH_2–dendrimer/TOABr–Pd NP)$_3$/NH_2–dendrimer colloids, as shown in Fig. 4b. Although the infiltration depth of TMB molecules into the multilayer shell in the oxidation reaction is closely related to the shell thickness, the shell porosity, and the diffusion time of TMB molecules, our results showed that the porous and ultrathin shells composed of globular dendrimers and spherical NPs did not have a detectable effect on the degree of TMB oxidation in the given reaction time.

Additionally, we confirmed that the multicatalytic colloids with OA–TiO_2 NPs could be used as effective photocatalysts. As shown in Fig. 6b and S8,† the absorbance peak intensity (at 665 nm) of methylene blue (MB) was rapidly decreased by the photocatalytic activity of OA–TiO_2 NP-embedded colloids under UV-light irradiation at 365 nm.[50,53–55] With increasing UV irradiation time up to 180 min, approximately 70% of the MB molecules were degraded by the photocatalytic properties of the OA–TiO_2 NP-embedded multicatalytic colloids. Generally, when the TiO_2 NPs are irradiated by UV light equal to or greater than their intrinsic band-gap energy (approximately 3.2 eV),[55] electrons (e^-) are excited from the valence band (VB) into the conduction band (CB), and holes (h^+) are created in the VB. In this case, the excited electrons can react with O_2 molecules, leading to the formation of the hydroxyl radical ($OH^•$); and the resulting holes (h^+) also participate in the formation of $OH^•$ through the adsorption of hydroxyl anions. These generated hydroxyl radicals are sufficiently reactive to decompose the MB molecules adsorbed onto the surface of the catalysts. We also observed that the photocatalytic degradation of multicatalytic colloids followed first-order kinetics, as predicted by the Langmuir–Hinshelwood model (see the inset of Fig. 6b).[54] In contrast, in the case of an MB aqueous solution without multicatalytic colloids, we did not observe any notable photocatalytic reactions.

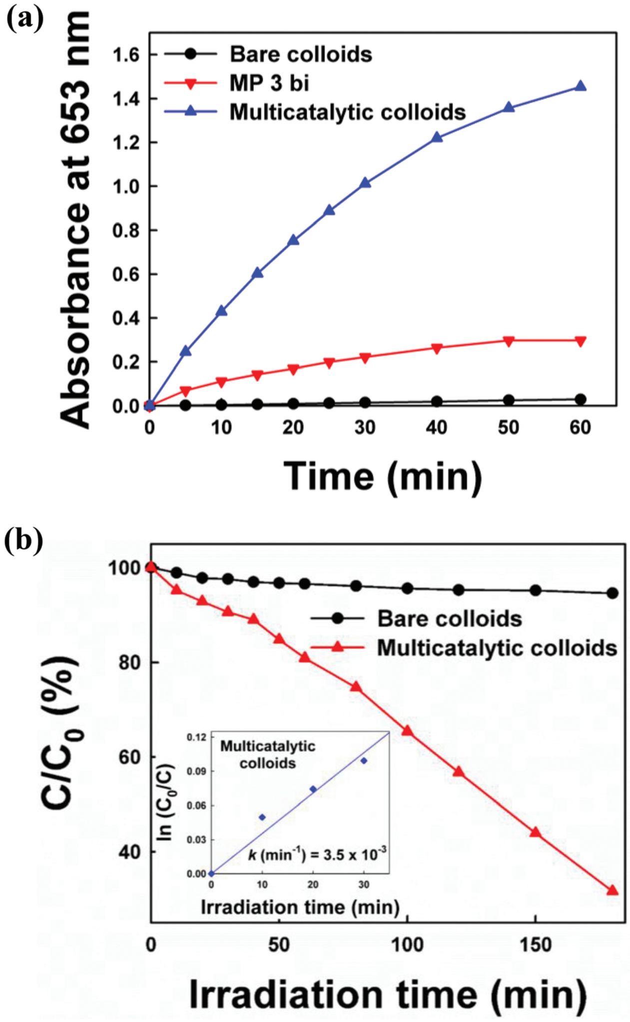

Fig. 6 (a) Time-dependent absorbance evolution (at 653 nm) of TMB in various reaction systems: (i) bare colloids, (ii) (NH_2–dendrimer/OA–Fe_3O_4 NP)$_3$ multilayer-coated colloids, and (iii) multicatalytic colloids at 40 °C. Three different types of reaction systems in a 0.1 M NaOAc buffer solution containing 0.3×10^{-3} M TMB and 0.1 M H_2O_2. (b) Photodegradation of methylene blue (MB) under UV-light irradiation (at 365 nm) using bare colloids and multicatalytic colloids. Here, the outermost layer of the multicatalytic colloids consisted of NH_2–dendrimers to disperse the assembled colloids and to induce catalytic reactions in water (*i.e.*, SiO_2/(NH_2–dendrimer/OA–Fe_3O_4 NP)$_3$/(NH_2–dendrimer/TOABr–Pd NP/NH_2–dendrimer/OA–TiO_2 NP)$_3$/NH_2–dendrimer).

This journal is © The Royal Society of Chemistry 2016

Published on 19 October 2015. Downloaded by Korea University on 26/03/2016 04:39:26.

We also investigated the Sonogashira coupling reaction of aryl iodide using multicatalytic colloids with TOABr–Pd NP layers (*i.e.*, SiO_2/(NH_2–dendrimer/OA–Fe_3O_4 NP)$_3$/(NH_2–dendrimer/TOABr–Pd NP/NH_2–dendrimer/OA–TiO_2 NP)$_3$) in organic media. As shown in Table 2, the high yield (99%) of diphenylacetylene produced by multicatalytic colloids was no different from that obtained from the (NH_2–dendrimer/TOABr–Pd NP)$_3$ colloids shown in Table 1. Furthermore, we calculated turnover numbers (TONs) of multicatalytic colloids in the Sonogashira coupling reaction. Given that the amount of Pd NPs embedded within multicatalytic colloids was measured to be 1.7 wt% by ICP-MS analysis, the TONs was approximately 474. It should be here noted that these values were higher than those reported by other research groups.[5,56,57] For example, the Hyeon group reported that the TON of the Sonogashira reaction based on recyclable catalytic colloids was calculated to be 33.[5] These results strongly support the conclusion that, as already indicated in Fig. 6a, small organic molecules can easily penetrate into ultrathin multilayer shells with a porous structure.

To further show the benefit of our multicatalytic colloids, we performed two different kinds of catalytic reactions (*i.e.*, peroxidase-like activity by Pd NPs and photocatalytic degradation by TiO_2 NPs) using the multicatalytic colloids (*i.e.*, SiO_2/(NH_2–dendrimer/OA–Fe_3O_4 NP)$_3$/(NH_2–dendrimer/TOABr–Pd NP/NH_2–dendrimer/OA–TiO_2 NP)$_3$/NH_2–dendrimer) dispersed in the same aqueous solution. First, we prepared the mixture solution containing MB (15 ppm) and 0.3 mM *o*-phenylenediamine (OPD) in the presence of 100 mM H_2O_2 (see Experimental).[58] When the UV light (at 365 nm) was irradiated on the mixture solution at 40 °C, the absorbance peak of MB (at 665 nm) was decreased, however the absorbance peak intensity (at 425 nm) occurring from OPD oxidation was rapidly increased with increasing reaction time (see the ESI, Fig. S9†). That is, the hydroxyl radicals generated by both the catalytic reactions caused MB to be colorless products (*i.e.*, photodegradation reaction by TiO_2 NPs), and on the other hand oxidized OPD to be yellow materials (*i.e.*, peroxidase-like activity by Pd NPs) at the same time. These results evidently showed that our approach could be effectively applied to the multicatalytic colloids with cooperative catalytic properties.

3.5. Recycling stability of multicatalytic colloids

Generally, on an industrial scale, it is not easy to collect the catalysts from a reaction mixture after reaction completion. Nevertheless, the recovery and reuse of precious metal catalysts are especially important because of the high costs of the catalysts and/or the possibility of heavy metal contamination in pharmaceutical products for human use.[59] In this regard, our approach has a notable advantage in that due to the densely packed OA–Fe_3O_4 NP layers (Fig. 7a), LbL-assembled multicatalytic colloids can be easily collected and recycled with a magnet. The magnetization of the multicatalytic colloids containing 8 nm OA–Fe_3O_4 NPs was also examined by super-

Table 2 Sonogashira coupling reaction of aryl iodide using (NH_2–dendrimer/OA–Fe_3O_4 NP)$_3$/(NH_2–dendrimer/TOABr–Pd NP/NH_2–dendrimer/OA–Fe_3O_4 NP)$_3$ multilayer-coated colloids[a]

Entry	Substrate (Ar–I)	Terminal alkyne (phenylacetylene)	Coupling product	Yield[b] [%]
1[c]	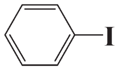	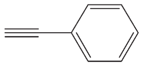	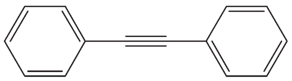	17
2	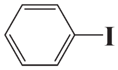	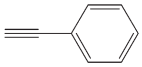	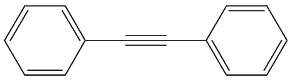	99
3[c]	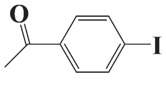	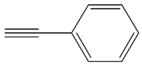	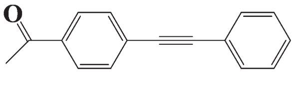	1.3
4	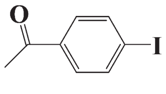	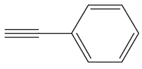	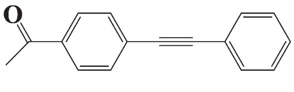	81
5[c]	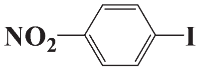	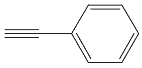	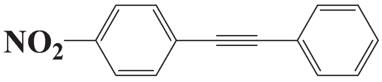	46
6	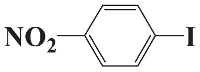	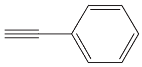	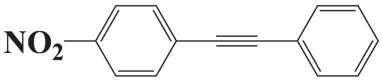	99

[a] Reaction conditions: Ar–I (4 mmol), phenylacetylene (5.2 mmol), CuI (5.0 mol%), (NH_2–dendrimer/OA–Fe_3O_4 NP)$_3$/(NH_2–dendrimer/TOABr–Pd NP/NH_2–dendrimer OA–Fe_3O_4 NP)$_3$ multilayer-coated colloids (50 mg), and TEA (20 mL) at 88 °C under argon. [b] Yields determined by GC-MS analysis. [c] Without catalysts to compare with the catalytic ability of Pd-contained multicatalytic colloids.

Published on 19 October 2015. Downloaded by Korea University on 26/03/2016 04:39:26.

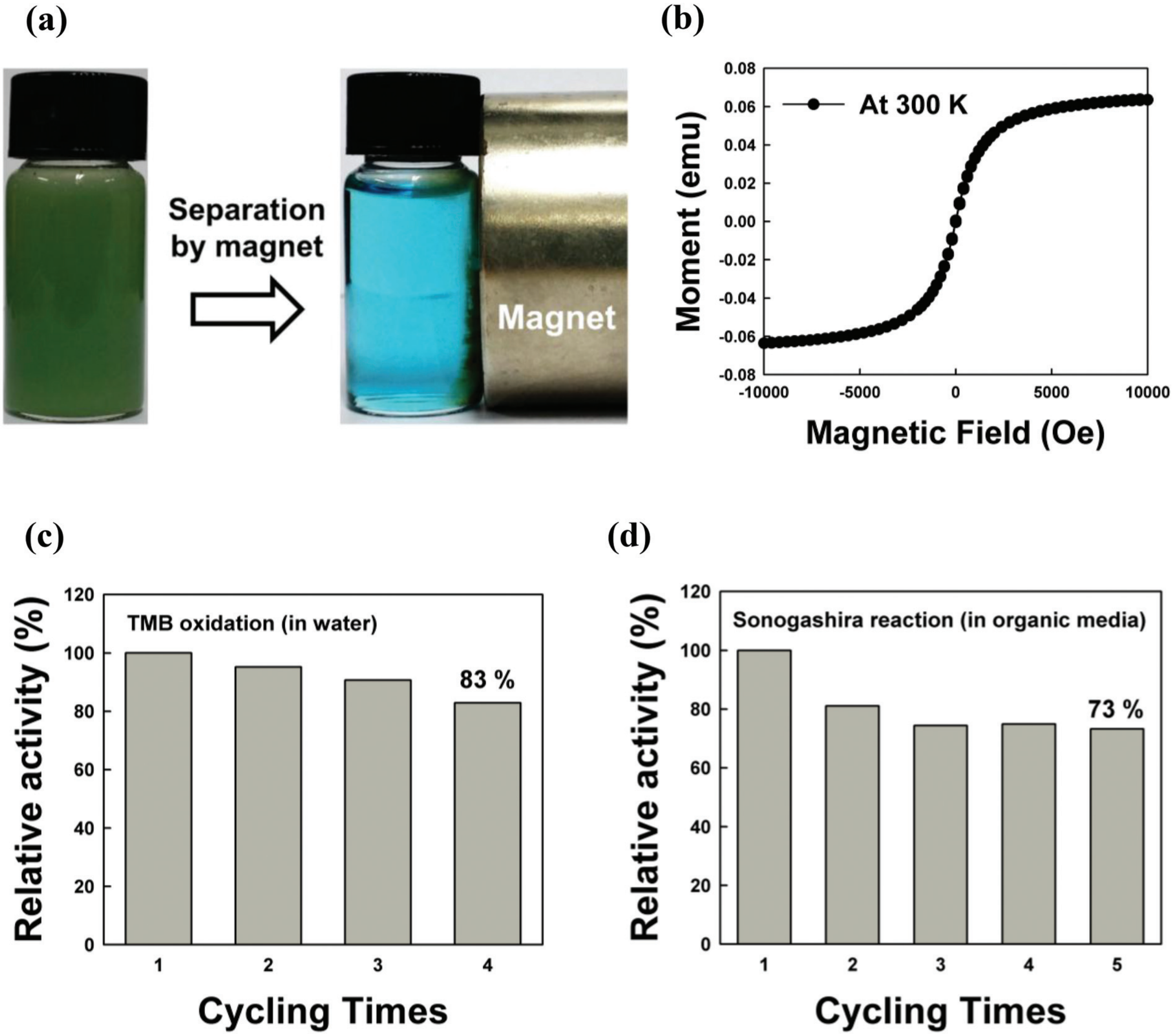

Fig. 7 (a) Photographs of multicatalytic colloids with magnetic responsive properties in the TMB-oxidation system. (b) Magnetism curve of the multicatalytic colloids measured at room temperature. Reusability of the multicatalytic colloids: (c) TMB oxidation in water and (d) Sonogashira reaction in triethylamine (TEA). Here, the structure of the multicatalytic colloids was SiO_2/(NH_2–dendrimer/OA–Fe_3O_4 NP$)_3$/(NH_2–dendrimer/TOABr–Pd NP/NH_2–dendrimer/OA–TiO_2 NP$)_3$.

conducting quantum interference device magnetometry (SQUID). The magnetization curves of the multicatalytic colloids measured at room temperature (T = 300 K) were reversible without coercivity, remanence or hysteresis, implying typical superparamagnetic behavior (Fig. 7b). More detailed magnetic properties of the multicatalytic colloids are presented in Fig. S10.†

Based on these magnetic properties, we examined the recycling stability of multicatalytic colloids during repeated catalytic reaction (Fig. 7c and d). First, after completion of TMB oxidation, the multicatalytic colloids were magnetically separated from the reaction medium, washed thoroughly with DI water several times, and then reused in another reaction vessel under the same conditions. Although the TMB-oxidation activities of the multicatalytic colloids gradually decreased with increasing recycling iteration, the catalytic activity in the fourth reaction was maintained at up to 83% of the activity in the first reaction. Additionally, this recycling stability of the multicatalytic colloids was also observed in the Sonogashira coupling reaction in organic media, as well as in TMB oxidation in aqueous media. The yield of 1-nitro-4-(phenylethynyl)-benzene in the presence of the multicatalytic colloids was measured to be approximately 73% in the fifth reaction (Fig. 7d).

We also investigated the leaching amount of Pd NPs after the catalytic reactions using ICP-MS analysis. First, in the case of the TMB oxidation in aqueous media, the leaching amount of Pd NPs after first and third run was measured to be approximately 0.21 and 0.06 ppm, respectively. Similarly, the leaching amount of Pd NPs after the first and third run Sonogashira reaction was 0.47 ppm and 0.10 ppm, respectively. Considering that all the Pd leaching values measured from recycling tests of TMB and Sonogashira reactions were extremely low, the gradual decrease of catalytic activity with increasing recycling

This journal is © The Royal Society of Chemistry 2016

Published on 19 October 2015. Downloaded by Korea University on 26/03/2016 04:39:26.

tests was mainly caused by the partial loss of the multicatalytic colloids themselves in the recovery process rather than the leaching phenomena of Pd NPs. However, it should be noted that this recycling yield was still highly relative to those previously reported by other research groups.[57] For example, it was reported that the Sonogashira coupling reaction yield of catalytic colloids coated by Fe_3O_4 NPs and Pd NPs decreased to 17% in the fourth recycling reaction because of the relatively easy detachment of Pd NPs from the SiO_2 colloids.[5] Based on these results, it is reasonable to conclude that the high recycling stability of the multicatalytic colloids shown in our study can be attributed to the formation of covalent bonds between the NH_2–dendrimers containing multiple binding sites and the metal (or metal oxide) NPs within the LbL-assembled multilayer.

4. Conclusions

We have demonstrated that recyclable multicatalytic colloids, which can be used in various solvent media, can be easily prepared using LbL assembly and that their catalytic activity can be controlled by multilayer design, including the composition and the bilayer number of the catalytic NPs. Furthermore, the ligand-exchange-induced LbL assembly between the hydrophobic ligands loosely bound to the surface of the NPs (*i.e.*, TOABr–Pd, OA–TiO_2, and OA–Fe_3O_4 NPs) and the NH_2-functionalized dendrimers notably enhanced the recycling stability of the multicatalytic colloids in aqueous and organic media. Although we demonstrated that single colloids (*i.e.*, SiO_2/(NH_2–dendrimer/OA–Fe_3O_4 NP$)_3$/(NH_2–dendrimer/TOABr–Pd NP/NH_2–dendrimer/OA–TiO_2 NP$)_3$) can enable multicatalytic activity in several notable processes (*i.e.*, TMB oxidation by TOABr–Pd NPs, photocatalysis by OA–TiO_2 NPs, and the Sonogashira coupling reaction by TOABr–Pd NPs), it should be noted that various other catalytic NPs with desired functionalities could be easily integrated with the colloids and that their catalytic properties could be further improved by increasing the NP layer number. Considering that various metal or metal oxide NPs synthesized by organic fatty acid or ammonium-based ligands can be directly LbL-assembled with NH_2-functionalized dendrimers, our approach provides a basis for exploiting and designing high-performance recyclable catalysts with scalable functionalities.

Acknowledgements

This work was supported by the National Research Foundation (NRF) grant funded by the Ministry of Science, ICT & Future Planning (MSIP) (NRF-2015R1A2A1A01004354).

References

1 M. Giersig, T. Ung, L. M. Liz-Marzan and P. Mulvaney, *Adv. Mater.*, 1997, **9**, 570.
2 F. Caruso, R. A. Caruso and H. Möhwald, *Science*, 1998, **282**, 1111.
3 F. Caruso and C. Schüler, *Langmuir*, 2000, **16**, 9595.
4 A. Voigt, H. Lichtenfeld, G. B. Sukhorukov, H. Zastrow, E. Donath, H. Bäumler and H. Möhwald, *Ind. Eng. Chem. Res.*, 1999, **38**, 4037.
5 J. Kim, J. E. Lee, J. Lee, Y. Jang, S.-W. Kim, K. An, J. H. Yu and T. Hyeon, *Angew. Chem., Int. Ed.*, 2006, **45**, 4789.
6 L.-S. Lin, Z.-X. Cong, J.-B. Cao, K.-M. Ke, Q.-L. Peng, J. Gao, H.-H. Yang, G. Liu and X. Chen, *ACS Nano*, 2014, **8**, 3876.
7 Y. Yan, M. Björnmalm and F. Caruso, *ACS Nano*, 2013, **7**, 9512.
8 D. Walsh and S. Mann, *Nature*, 1995, **377**, 320.
9 O. M. Wilson, M. R. Knecht, J. C. Garcia-Martinez and R. M. Crooks, *J. Am. Chem. Soc.*, 2006, **128**, 4510.
10 F. Wang, C. Li, L.-D. Sun, H. Wu, T. Ming, J. Wang, J. C. Yu and C.-H. Yan, *J. Am. Chem. Soc.*, 2011, **133**, 1106.
11 H. G. Yang, C. H. Sun, S. Z. Qiao, J. Zou, G. Liu, S. C. Smith, H. M. Cheng and G. Q. Lu, *Nature*, 2009, **453**, 638.
12 M. Moreno, L. N. Kissell, J. B. Jasinski and F. P. Zamborini, *ACS Catal.*, 2012, **2**, 2602.
13 W. Wang, Y. Xu, D. I. C. Wang and Z. Li, *J. Am. Chem. Soc.*, 2009, **131**, 12892.
14 M. Feyen, C. Weidenthaler, F. Schüth and A.-H. Lu, *Chem. Mater.*, 2010, **22**, 2955.
15 S. Luo, F. Chai, L. Zhang, C. Wang, L. Li, X. Liu and Z. Su, *J. Mater. Chem.*, 2012, **22**, 4832.
16 R. Abu-Reziq, D. Wang, M. Post and H. Alper, *Chem. Mater.*, 2008, **20**, 2544.
17 X. Song and L. Gao, *J. Am. Ceram. Soc.*, 2007, **90**, 4015.
18 Y. Deng, T. C. Cai, Z. Sun, J. Liu, C. Liu, J. Wei, W. Li, C. Liu, Y. Wang and D. Zhao, *J. Am. Chem. Soc.*, 2010, **132**, 8466.
19 T. A. G. Silva, R. Landers and L. M. Rossi, *Catal. Sci. Technol.*, 2013, **3**, 2993.
20 G. Decher, *Science*, 1997, **277**, 1232.
21 P. Podsiadlo, A. K. Kaushik, E. M. Arruda, A. M. Waas, B. S. Shim, J. D. Xu, H. Nandivada, B. G. Pumplin, J. Lahann and A. Ramamoorthy, *Science*, 2007, **318**, 80.
22 J. Hong, N. J. Shah, A. C. Drake, P. C. Demuth, J. B. Lee, J. Chen and P. T. Hammond, *ACS Nano*, 2012, **6**, 81.
23 M. A. Correa-Duarte, A. Kosiorek, W. Kandulski, M. Giersig and L. M. Liz-Marzan, *Chem. Mater.*, 2005, **17**, 3268.
24 P. Schuetz and F. Caruso, *Chem. Mater.*, 2004, **16**, 3066.
25 J. Schmitt, G. Decher, W. J. Dressick, S. L. Brandow, R. E. Geer, R. Shashidhar and J. M. Calvert, *Adv. Mater.*, 1997, **9**, 61.
26 Y. Lvov and F. Caruso, *Anal. Chem.*, 2001, **73**, 4212.
27 S. Kidambi, J. Dai, J. Li and M. L. Bruening, *J. Am. Chem. Soc.*, 2004, **126**, 2658.
28 S. Bhattacharjee, D. M. Dotzauer and M. L. Bruening, *J. Am. Chem. Soc.*, 2009, **131**, 3601.
29 F. Zhang and M. P. Srinivasan, *Langmuir*, 2007, **23**, 10102.
30 N. Krasteva, I. Besnard, B. Guse, R. E. Bauer, K. Mullen, A. Yasuda and T. Vossmeyer, *Nano Lett.*, 2002, **2**, 551.

Published on 19 October 2015. Downloaded by Korea University on 26/03/2016 04:39:26.

31 Y. Ko, H. Baek, Y. Kim, M. Yoon and J. Cho, *ACS Nano*, 2013, **7**, 143.

32 S. Sun, *Adv. Mater.*, 2006, **18**, 393.

33 N. Miyaura and A. Suzuki, *Chem. Rev.*, 1995, **95**, 2457.

34 Á. Monlár, *Chem. Rev.*, 2011, **111**, 2251.

35 V. Etacheri, M. K. Seery, S. J. Hinder and S. C. Pillai, *Chem. Mater.*, 2010, **22**, 3843.

36 T. A. Kandiel, A. Feldhoff, L. Robben, R. Dillert and D. W. Bahnemann, *Chem. Mater.*, 2010, **22**, 2050.

37 S. Sun, H. Zeng, D. B. Robinson, S. Raoux, P. M. Rice, S. X. Wang and G. Li, *J. Am. Chem. Soc.*, 2004, **126**, 273.

38 D. I. Gittins and F. Caruso, *Angew. Chem., Int. Ed.*, 2001, **40**, 3001.

39 D. Pan, N. Zhao, Q. Wang, S. Jiang, X. Ji and L. An, *Adv. Mater.*, 2005, **17**, 1991.

40 G. Lawrie, I. Keen, B. Drew, A. Chandler-Temple, L. Rintou, P. Fredericks and L. Grøndahl, *Biomacromolecules*, 2007, **8**, 2533.

41 D. V. Leff, L. Brandt and J. R. Heath, *Langmuir*, 1996, **12**, 4723.

42 A. Kumar, S. Mandal, P. R. Selvakannan, R. Pasricha, A. B. Mandale and M. Sastry, *Langmuir*, 2003, **19**, 6277.

43 J. Choi and M. F. Rubner, *Macromolecules*, 2005, **38**, 116.

44 L. Gao, J. Zhuang, L. Nie, J. Zhang, Y. Zhang, N. Gu, T. Wang, J. Feng, D. Yang, S. Perrett and X. Yan, *Nat. Nanotechnol.*, 2007, **2**, 577.

45 L. Su, J. Feng, X. Zhou, C. Ren, H. Li and X. Chen, *Anal. Chem.*, 2012, **84**, 5753.

46 P. D. Josephy and R. P. Mason, *J. Biol. Chem.*, 1982, **257**, 3669.

47 Y. Niu, L. K. Yeung and R. M. Crooks, *J. Am. Chem. Soc.*, 2001, **123**, 6840.

48 R. Chinchilla and C. Nájera, *Chem. Rev.*, 2007, **107**, 874.

49 J. M. Pedersen, W. R. Bowman, M. R. J. Elsegood, A. J. Fletcher and P. J. Lovell, *J. Org. Chem.*, 2005, **70**, 10615.

50 J. Liu, H. Bai, Y. Wang, Z. Liu, X. Zhang and D. D. Sun, *Adv. Funct. Mater.*, 2010, **20**, 4175.

51 Z. Li, J. Gao, X. Xing, S. Wu, S. Shuang, C. Dong, M. C. Paau and M. M. F. Choi, *J. Phys. Chem. C*, 2010, **114**, 723.

52 G. Liu, C. Sun, L. Cheng, Y. Jin, H. Lu, L. Wang, S. C. Smith, G. Q. Lu and H.-M. Cheng, *J. Phys. Chem. C*, 2009, **113**, 12317.

53 J. S. Lee, K. H. You and C. B. Park, *Adv. Mater.*, 2012, **24**, 1084.

54 A. T. Kuvarega, R. W. M. Krause and B. B. Mamba, *J. Phys. Chem. C*, 2011, **115**, 22110.

55 L.-L. Tan, S.-P. Chai and A. R. Mohamed, *ChemSusChem*, 2012, **5**, 1868.

56 H. Li, Z. Zhu, H. Li, P. Li and X. Zhou, *J. Colloid Interface Sci.*, 2010, **349**, 613.

57 A. Corma, H. García and A. Primo, *J. Catal.*, 2006, **241**, 123.

58 W. He, X. Wu, J. Liu, X. Hu, K. Zhang, S. Hou, W. Zhou and S. Xie, *Chem. Mater.*, 2010, **22**, 2988.

59 C. E. Garrett and K. Prasad, *Adv. Synth. Catal.*, 2004, **346**, 889.

This journal is © The Royal Society of Chemistry 2016